

**RIGA TECHNICAL UNIVERSITY**  
Faculty of Transport and Mechanical Engineering  
Institute of Mechanics

**Arturs Macanovskis**

Doctoral study program „Engineering Technology, Mechanics and Mechanical Engineering”

**SHORT FIBER COMPOSITE INTERNAL GEOMETRY  
INFLUENCE ON THE MATERIAL’S LOAD BEARING  
CAPACITY AND STRENGTH**

**Summary of Thesis**

Scientific supervisor  
Dr.sc.ing. professor  
Andrejs KRASNIKOVS

RTU Press

Riga 2014

UDK 691.328:620.17(043.2)

Ma 022 s

Macanovskis A. Short fiber composite internal geometry influence on the material's load bearing capacity and strength.-R.: RTU Publishing House, 2014. – 29 lpp.



*This work has been supported by the European Social Fund within the project «Support for the implementation of doctoral studies at Riga Technical University».*

**ISBN 978-9934-10-548-7**

**THE DOCTORAL THESIS IS PROMOTED FOR OBTAINING THE ENGINEERING  
SCIENCE DOCTOR'S DEGREE IN RIGA TECHNICAL UNIVERSITY**

The doctoral thesis for obtaining the engineering science (architecture, chemistry, economics, physics) doctor's degree will be publicly presented on 30 May at 14<sup>00</sup> 2014, in the Faculty of Mechanics of the Riga Technical University, Ezermalas street 6, room 302.

**OFICIAL REVIEWERS**

Professor Dr.sc.ing., Igors Tipāns  
Foreign Students Department director  
Riga Technical University

Professor Dr. sc. ing. Aleksandrs Korjakins  
Department of Building Materials and Products, Head of department  
Riga Technical University

Senior researcer, PhD. Heiko Herrmann  
Centre for Nonlinear Studies, Department of Mechanics and Applied Mathematics, Institute of Cybernetics at Tallinn University of Technology

**CONFIRMATION**

I confirm that I have developed this doctoral thesis that has been submitted for reviewing to Riga Technical University in order to obtain the engineering sciences doctor's degree. The doctoral thesis has not been submitted to any other university with the goal of obtaining a scientific degree.

Arturs Macanovskis .....(Signature)

Date: 21.04.2014.

The doctoral thesis has been prepared in English language, it contains an introduction, 5 chapters, conclusions, 12 appendixes, list of references, 165 drawings and illustrations, in total 164 pages. The list of references includes 85 titles.

## Contents

GENERAL DESCRIPTION OF THESIS.....	5
The topicality of the theme.....	5
The objectives of the thesis.....	5
Research tasks.....	5
Scientific novelty of the thesis.....	6
Practical value of the thesis.....	6
Research results determined in the thesis.....	6
Approbation.....	7
Publications.....	8
CONTENT OF THE THESIS.....	9
First chapter.....	9
Second chapter.....	9
Third chapter.....	15
Fourth chapter.....	21
Fifth chapter.....	23
CONCLUSIONS.....	28
REFERENCES.....	28

## **GENERAL DESCRIPTION OF THESIS**

### **The topicality of the theme:**

Creation of new sustainable and safe structures in the building industry (skyscrapers, bridges, tunnels and others) is impossible without novel construction materials use with high and superior features.

During the recent 20 years new materials have been elaborated in the construction industry that has radically new properties. These are self-compacting, high-strength and highly performance concretes. Materials are characterized by high and ultra-high compression strength. At the same time few disadvantages can be mention speaking about them. The most important among them is the increase of their fragility, as well as specific explosive behavior under the impact of high temperature and fire. The most important way how to overcome the mentioned difficulties is the use of short fibers, dispersed in the concrete body. Introduction of short steel (polymeric, nonmetallic synthetic etc.) fibers into the volume of material leads to appearance of new mechanic features. Impact resistance, resistance to rupture, as well as fire resistance can be significantly increased. Use of short fibers in the concrete in average and high concentrations may lead to full rejection of traditional reinforcement use. Thus the study of micromechanics, nanomechanics and macro mechanics of materials is important, necessary and topical.

### **The objectives of the thesis:**

By systematic investigation of the short fiber composite fracture micromechanics, to develop recommendations for improvement of fiberconcrete production technologies, obtaining materials with higher bearing capacity and predictability of mechanic properties at the cracking stage.

### **Research tasks:**

1. Study the mechanics of breaking of fibercomposite structures and micromechanics during the loading procedure from the beginning of crack formation to the structure's full loss of bearing capacity.

1.1. Experimental study of fiber pull-out micromechanics:

1.1.1. Steel fiber pull-out of the concrete;

1.1.2. Polymeric macro fiber pull-out of the concrete;

1.1.3. Polymeric micro fiber pull-out of the concrete.

2. Experimental study of fibers distribution (by location and orientations) in the place of macro-crack development.

2.1. Define visually the pull-out fibers ends locations, pull-out end's length and orientations to the crack's plane.

2.2. Perform the X-ray analysis of samples.

3. Study theoretically fibers distribution (by locations and orientations) in the place of macro-crack development.

3.1. Using the statistical Monte-Carlo method, model fibers locations and orientations in the sample.

4. Develop and study the inhomogeneous (layered) fibercomposite (fiberconcrete) production technologies.
5. Study the development procedure of one macro-crack in the inhomogeneous fiberconcrete prism.
  - 5.1. Produce and experimentally study the crack development in the layered fiberconcrete with steel fibers.
  - 5.2. Compare the bearing capacity of homogeneous and inhomogeneous prisms at bending.

#### **Scientific novelty of the thesis:**

The thesis presents a study of micromechanics of steel and polymeric fibers pull-out from the concrete matrix. Experimentally the fibers distribution on the crack's surface was studied, as well as their spatial orientations in bending of fiberconcrete beams. Using the X-ray analysis a confirmation was received that there are "weak" areas – the areas with decreased content of fibers and their undesirable orientation. Detailed macroscopic study of the canal's surface left by the pulled steel fiber out of the concrete matrix was performed. Erosion of the matrix's surface in the canal of the pulled out fiber was found, which leads to formation of sand "congestion" during pull-out procedure. Numerical modeling of filling of the mould by fiberconcrete mix was performed when casting the beam. The areas of high gradients of vertical speed were detected. The beams consisting of layers of fiberconcrete with different concentration of fibers in them were created. A possibility of increasing the bearing capacity under bending was shown, in case of concentration of fibers in the layers (non-homogeneous fiberconcrete) if compared to fiberconcrete beams containing chaotic arrangement of fibers along the volume.

#### **Practical value of the thesis:**

The results of work have practical value when creating high-tensile fiberconcrete and ferroconcrete structures. Basing on the performed modeling it is easy to predict the required fiber concentration in case of different applied loads acting on structure. Use of layered fiberconcrete structure is proposed. The mechanisms of the bearing capacity of fiberconcrete at different fiber concentration have been stated.

#### **Research results determined in the thesis:**

- A) results of experimental study of fiber arrangement (by the place and orientation in the weak section of the bent beam) in the crosssection, which is coincide with the main crack.
- B) results of numerical modeling (predictions of "weak " sections during the fiberconcrete casting as a result of areas with high value of flow speed gradients)
- C) results of numerical modeling of fiberconcrete beam behavior under the load (modeling of bearing capacity)
- D) results of experimental study of the bearing capacity of layered fiberconcrete beams.

## Approbation:

- RTU 50. Studentu zinātniskās un tehniskās konferences (Rīga, Latvija, 2009)
- RTU 51. starptautiskā zinātniskā konference: „Inženiertehnika, mehānika un mašīnbūve” „**Šķiedru sadalījums pa apjomu īso šķiedru kompozītos**” (Rīga, Latvija, 2010)
- RTU 51. Studentu zinātniskās un tehniskās konferences (Rīga, Latvija, 2010)
- Sixteenth international conference. Mechanics of composite materials. (Riga, Latvia, 2010)
- „Latvijas betona savienība” XX zinātniski tehniskajā konference. „**Nehomogēno fibrobetonu iekšējā struktūra un to slodzes nestspēja**” (Rīga, Latvija, 2010)
- World Academy of Science, Engineering and Technology „**Post – cracking behaviour of high strength fiber concrete prediction and validation**” (Venice, Italy, 2011)
- RTU 52. starptautiskā zinātniskā konference: „Inženiertehnika, mehānika un mašīnbūve” „**Īso šķiedru kompozītu sabrukšanas stohastiska modelēšana**” (Rīga, Latvija, 2011)
- RTU 52. starptautiskā zinātniskā konference: „Būvzinātne” „**Nehomogēna fibrobetona struktūra un stiprība**” (Rīga, Latvija, 2011)
- RTU 52. Studentu zinātniskās un tehniskās konferences. „**Mehānisko testu salīdzināšana. Prizmu četru punktu liece, plātņu saspiešana**” (Rīga, Latvija, 2011)
- RTU 52. Studentu zinātniskās un tehniskās konferences. „**Iekšējās struktūras analīze un modelēšana fibrobetonos**”(Rīga, Latvija, 2011)
- RTU 53. Studentu zinātniskās un tehniskās konferences. „**Nesimetriskas formas šķiedras orientēšana viskozā šķidrums plūsmā**” (Rīga, Latvija, 2011)
- RTU 53rd International Scientific Conference. Dedicated to the 150th anniversary and the 1st congress of world engineers and Riga polytechnical institute / RTU Alumni. A.Krasnikovs, A.Macanovskis, V.Lusis, E.Macanovskis. „**Stress distribution along the crack in cracked bended fiber concrete beam**”(Riga, Latvia, 2012)
- RTU 53rd International Scientific Conference. Dedicated to the 150th anniversary and the 1st congress of world engineers and Riga polytechnical institute / RTU Alumni. A.Krasnikovs, O.Kononova, A.Machanovskis, A.Losevs, A.Galushchaka. Presentation: „**About possibility to predict fibers orientation and distribution in viscous flow**” (Riga, Latvia, 2012)
- „Mechanics of composite materials”, Seventeenth international conference, (Riga, Latvia, 2012)
- „LATVIAN CONCRETE ASSOCIATION”, XXI scientific and technical conference of Latvian Concrete Association. „**Tensile strength dependance on fibers distribution in fiberconcrete**”. Riga, Latvia, 2012)
- RTU 54. starptautiskā zinātniskā konference, Sekcija: Transporta un mašīnzinību fakultātē. „**Fibru izvietošanas kārtība fibrobetonos**” (Rīga, Latvija, 2013)
- “Civil engineering `13” 4<sup>th</sup> International Scientific Conference „**Polymer fiber pull out experimental investigation**” (Jelgava, Latvia, 2013)
- „Latvijas betona savienība” XXII zinātniski tehniskajā konference. „**Fibrobetona iekšējās struktūras veidošana**”, (Rīga, Latvija, 2013)

## Publications:

- Krasnikovs A., Kononova O., Eiduks M., Kalinka J., Kharkova G., Galushchak A., **Machanovsky A.**, *„Fiber orientation in viscous fluid flow with and without vibration”*. „Journal of Vibroengineering” Volume 12, Issue 4, ISSN 1392-8716, Kaunas, Lithuania, December 2010.g, pp. 523-532.
- Krasnikovs, A. Khabbaz, A. Galushchak, A. **Machanovskis A.** *„Fibre Reinforced Concrete (FRC) (with Glass, Steel and Carbon Fibres) Strength”*. Proceedings of XXI Nordic Concrete Research Symposium, no.43 1/2011, Hämeenlinna, Finland 2011, pp. 407-410
- Krasnikovs A., Khabbaz A., Telnova I., **Machanovsky A.**, Klavinsh J.. *Numerical 3D Investigation of Non-Metallic (Glass, Carbon) Fiber Pull-out Micromechanics (in Concrete Matrix)*. Scientific Journal of Riga Technical University. “Transport and engineering”. Sērija 6, Sējums 33, Rīga 2010; pp. 103 – 108
- Krasnikovs A., Kononova O., Khabbaz A., Machanovsky E., **Machanovsky A.** *„Post – cracking behaviour of high strength fiber concrete prediction and validation”*. World Academy of Science, Engineering and Technology, ISSUE 59, pISSN 2010-376X, eISSN 2010-3778, Venice, Italy, November 2011.g. pp. 988 – 992
- Krasnikovs A., Kononova O., Khabbaz A., Machanovsky E., **Machanovsky A.** *„Post – Cracking Behavior of High Strength (Nano Level Designed) Fiber Concrete Prediction and Validation”*. Nanotechnology in Construction 4th International Symposium”, Agios Nikolaos, Crete, Greece, May 20-22, 2012, pp.1-6
- A.Krasnikovs, O.Kononova, **A.Machanovsky**, A.Khabbaz. *„Pull – out Micro-mechanism for Fibers in Concrete”*. Ecm15 - 15th european conference on composite materials, Venice, Italy, 24-28 June 2012 - ISBN 978-88-88785-33-2, pp.1-8
- Krasnikovs A., **Machanovskis A.**, Lūsis V., Lapsa V., Zaharevskis V. and Machanovskis E. *„Short fibers distribution investigation in fiber concrete”*. Mechanical Engineering and Mechanics. Scientific Works of Riga Technical University. ISBN 978-9984-9990-7-4. 2012.g. pp.54-62.
- Kononova O., Lūsis V., Galuščaka A., Krasnikovs A., **Mačanovskis A.**, *„Numerical Modeling of Fiber Pull-Out Micromechanics in Concrete Matrix Composites”*. Journal of Vibroengineering, Vol.14, Iss.4, ISSN 13928716, 2012, pp.1852.-1861.
- Lūsis V., Harjkova G., **Mačanovskis A.**, Kononova O., Krasnikovs A. *„Fracture of Layered Fiberconcrete with Non-Homogeneous Fiber Distribution”*. In: Proceedings of 12th International Scientific Conference “Engineering for Rural Development”, Latvia, Jelgava, 23-24 May, ISSN: 16913043, 2013. Jelgava: 2013, pp.273-277.
- **Macanovskis A.**, Zaharevskis V., Krasnikovs A., *„Non-destructive evaluation of fibers orientation in fiberconcrete prism”*, „Civilengineering`13” 4<sup>th</sup> International Scientific Conference, Volume 4, Part 1, ISSN 2255-7776 print, ISSN 2255-8861 online, pp. 233 – 239
- **Macanovskis A.**, Lūsis V., Krasnikovs A., *„Polymer fiber pull out experimental investigation”*, „Civilengineering`13” 4<sup>th</sup> International Scientific Conference, Volume 4, Part 1, ISSN 2255-7776 print, ISSN 2255-8861 online, pp. 104 - 111

## CONTENT OF THE THESIS

**First chapter** begins with literature review, where the necessity for study of mechanics and micromechanics of single fiber's behavior in fiberconcrete is justified. Also is emphasized importance to investigate the arrangement and orientation of fibers inside the beam, during it's cracking under bending loads. Cracking means an appearance of the main crack is crossing the beam and it's opening under the load by slow pull-out of fibers from the crack's flanks. Considered such subsections how: short description of fiberconcrete, analysis of crack's internal structure, methods of determination of fiber orientation, study of orientation of fiber distribution by method of cutting of samples into parts, method of finding fiber orientation with the help of X-ray and modeling of pull-out of steel fiber from the concert matrix.

**Second chapter** are presented the results of experimental investigation of one single fiber pull-out of the concrete matrix. The canal's surface left in the concrete by the pulled out fiber was studied microscopically, as well as the single fibers (were embedded into concrete and were oriented at different angles towards the pull-out force) pull-out experimental results are were given (curves "force – length of pull-out fiber from the concrete matrix). Experiments were performed using fibers of different length, diameter and material (steel fibers, polymeric fibers). Concrete was used as the matrix.

Pull-out of one polymeric synthetic fiber that is 30 mm long and has a diameter of 0.55 mm out of the concrete matrix:

Considering the PSF (see Fig.1.1.), orientated at an angle of  $90^\circ$  to the crack's surface, we can see that there are fine concrete particles along the whole surface of the fiber (see Fig.1.2.), which were impeded fiber's pull-out. The fiber's surface is shabby. The fiber's end proves that the fiber was broken.



Fig.1.1. Polymeric synthetic fiber at an angle of  $90^\circ$  pull-out of the concrete (under microscope)

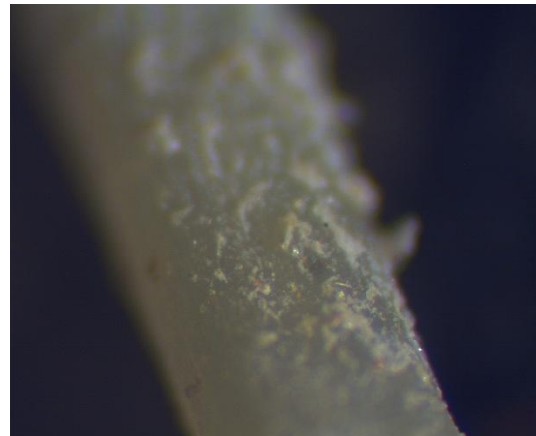


Fig.1.2. Fiber's surface at an angle of  $90^\circ$

The diagram in Fig.1.3. shows comparison of the averaged value of energy, which is spent for fiber's pull-out (including the work for fiber's delamination from the matrix, its rupture and pull-out of the torn-apart "tail" of the fiber from the matrix, deforming it) at different inclination angles of the fiber. It should be noted that the fiber orientated at an angle of  $90^\circ$  spends the most energy during pull-out, virtually it is two times bigger.

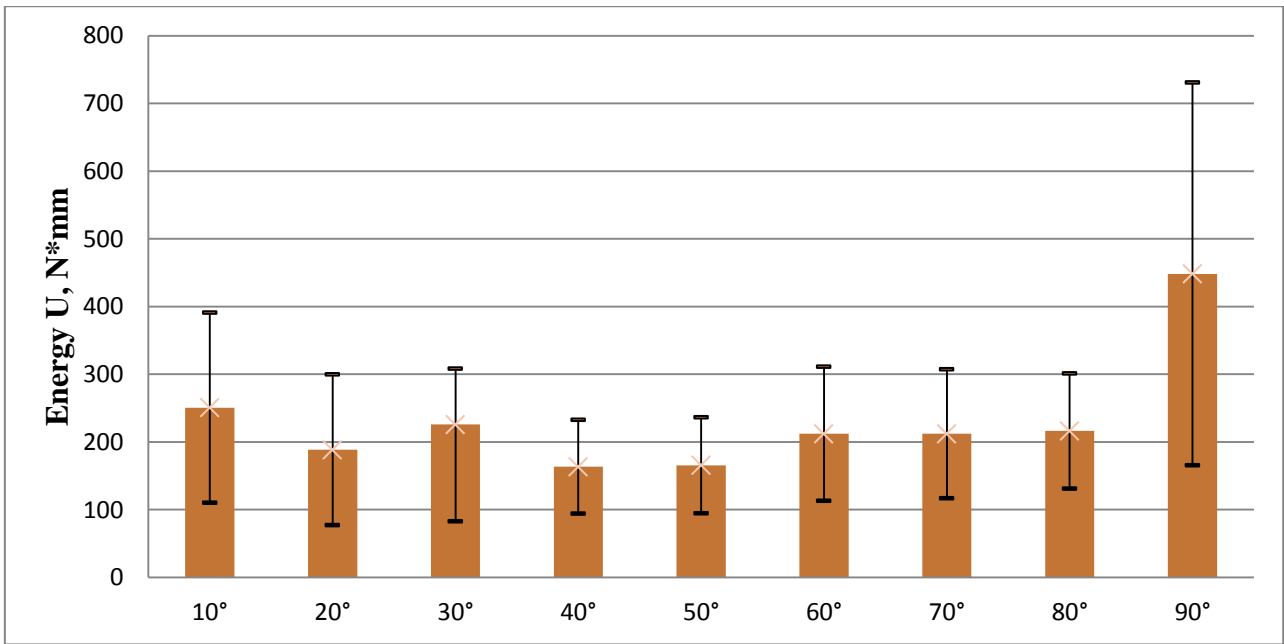


Fig.1.3. Energy of average value at the angles from 10° to 90°

Pull-out of macro PSF contained in the concrete at different angles towards the stretching force is shown in the Fig.1.4. The length of the pull-out “tail” of fiber from the concrete matrix at all orientations is less than a half of fiber’s length (15 mm), which proves that all fibers break.

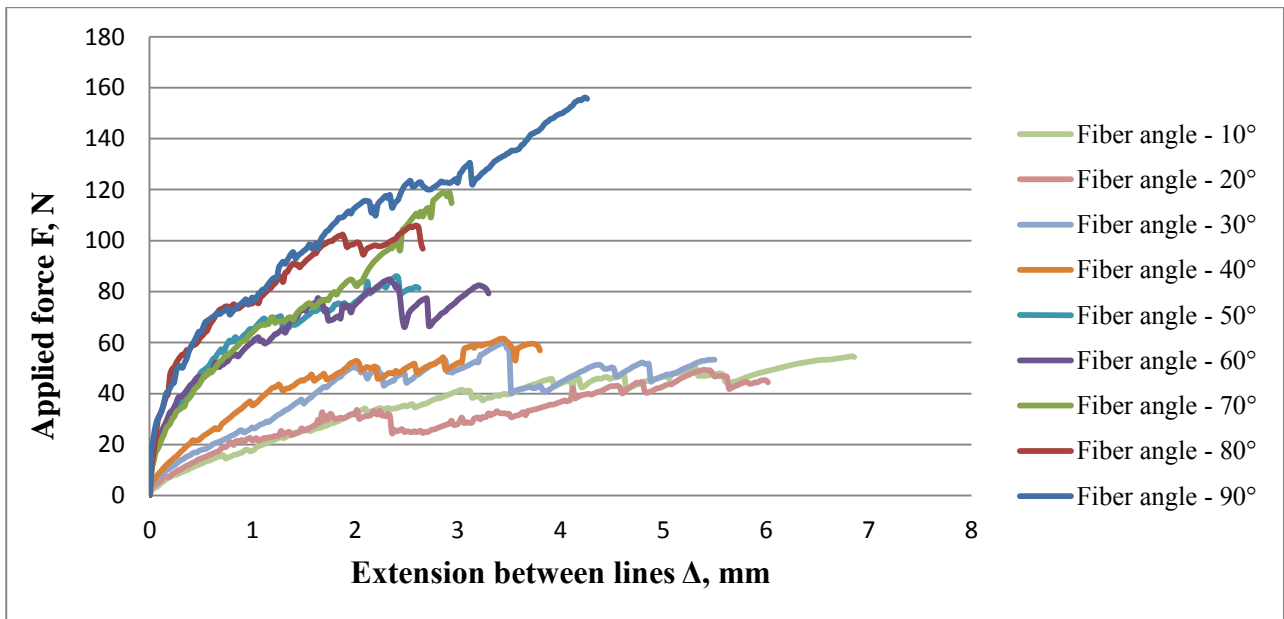


Fig.1.4. Average values for each angle, where F – applied force [N] and Δ - extension between lines [mm]

It is seen on the diagrams that PSF placed perpendicularly (90°) bears the highest load (equal to 155.620 N) than at other inclination angles. All diagrams show decline and growth of the applied force. At an angle of 90°, the force decline is explained by the fact that the pull-out macro PSF from the concrete matrix is exposed to gradual delamination and the delaminated part is accompanied by friction between the concrete and the fiber. As the PSF needs to spend larger load by every following delamination, a moment comes when the tested fiber stops delaminating and starts to

plastically deform in the end of the tested fiber (see Fig.1.1.). Deformation leads to decrease of fiber's diameter and the future rupture of the tested PSF. The average length of the released fiber's part (distance between the tapes) for samples at  $90^\circ$  is equal to  $\approx 4.1$  mm. At the angles from  $40^\circ$  to  $80^\circ$  we see the decline of the applied force, this is explained by the fact that the fiber not only gets delaminated, but it also destroys the surface of concrete matrix at the initial stage of pull-out. Destruction of concrete matrix increases by decrease of fiber's angle. Fibers at the angles of  $40^\circ$ - $80^\circ$  are subdivided into two different ruptures: 1) when the fiber suffers deformations, which lead to decrease of fiber's diameter and the fiber is torn; 2) when the PSF is exposed to the action of the cut at the concrete matrix at the expense of the arisen large tension between the tested fiber and the concrete (at this moment the fiber is not able to cut the concrete off anymore). The average length of the released PSF for samples at the angles of  $40^\circ$ - $80^\circ$  is equal to  $\approx 2.7 \div 3.6$  mm. Comparing to the average length for samples orientated at an angle of  $90^\circ$ , the loss constitutes  $\approx 10 \div 35\%$ . The angles of  $10^\circ$ - $30^\circ$  bear the least applied force. At these angles ( $10^\circ$ - $30^\circ$ ) the PSF shows only the fiber rupture caused by the cut at the concrete matrix. PSF placed at these angles give the highest released lengths of fiber from the concrete matrix, this is caused by the fact that the fiber in the output area easy destroys the concrete matrix. The length of the released fiber  $\approx 5.5 \div 6,86$  mm, which is by 25%-40% more than comparing to the angle of  $90^\circ$ , and by 35%-40% more comparing to the angles of  $40^\circ$ - $80^\circ$ . To reach the highest loads in the main crack, it is required to place fibers at  $90^\circ$ , and if we need to reach the maximum crack opening, then we need to reinforce the PSF at the angles of  $10^\circ$ -  $30^\circ$ .

Pull-out of one straight steel fiber with dimensions of 26 mm and diameter  $\approx 0.45 \div 0.5$  mm from the concrete matrix:

The diagram of pull-out of straight steel fiber at an angle of  $80^\circ$  is represented on Fig.1.5.

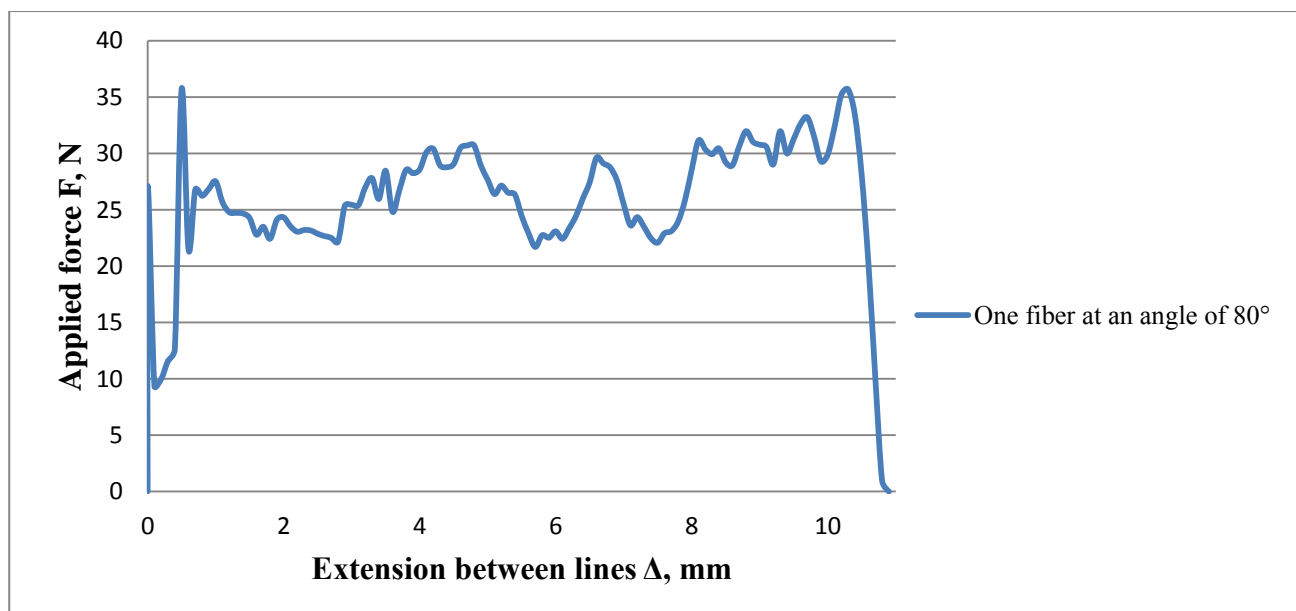


Fig.1.5. Extension of straight steel fiber orientated at an inclination of  $80^\circ$

It is seen in the image how the value of the applied force along the whole pull-out length changes within  $\approx 22 \div 32$  N. During microscopic study of the sample's surface (see Fig.1.6.), we see a trace of pull-out fiber of the concrete matrix. The trace looks like an even, undamaged surface, which means that the fiber, during the initial charge, destroys the concrete surface in the area of

fiber output (see Fig.1.7.) and there is no fiber friction (this is proved by broken-off particles during the experiment). The canal surface is wavy (see Fig.1.6.) and it is known that the fiber in this sample was orientated at an angle of inclination  $80^\circ$ . Thanks to this angle it is possible to define the length of trace (canal) left by the fiber after concrete destruction.

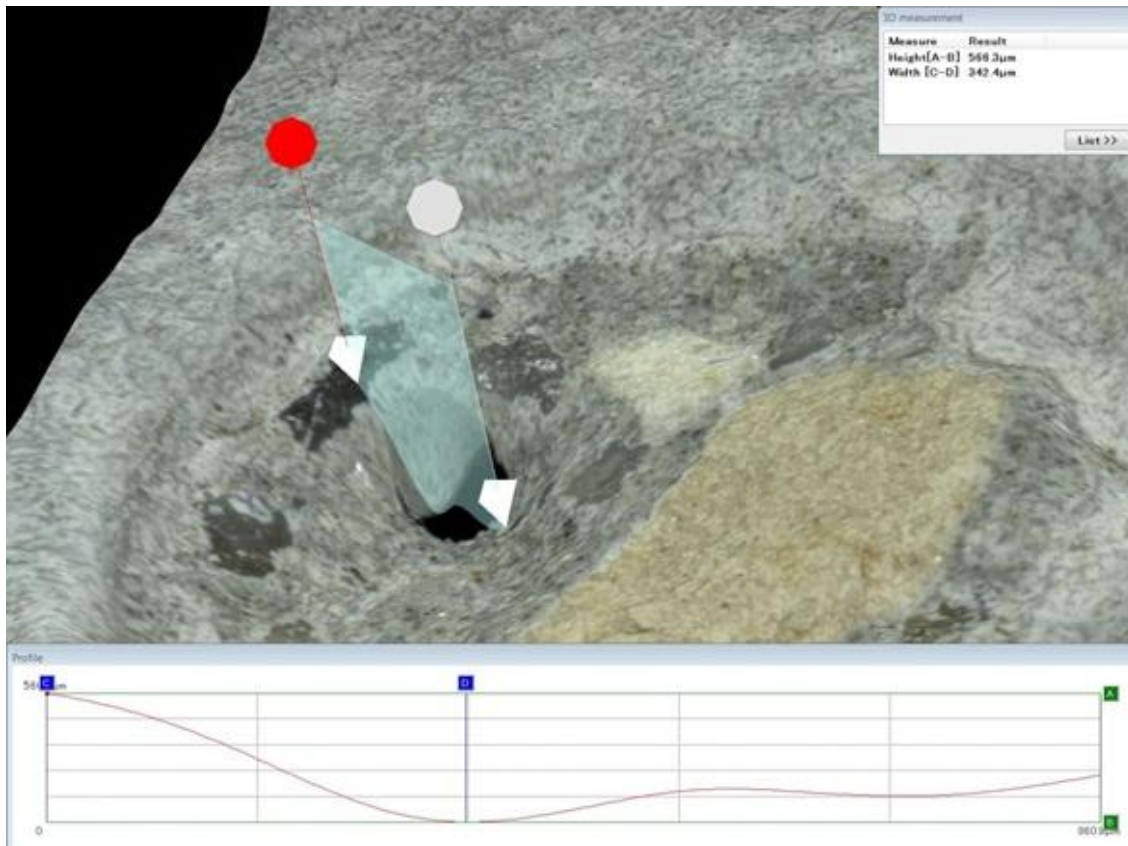


Fig.1.6. Analysis of canal surface in the sample N38 (3D)

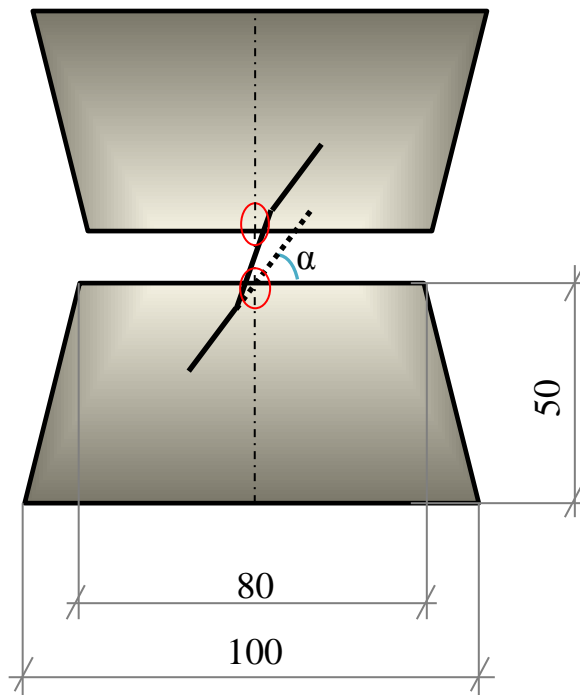


Fig.1.7. Areas of concrete spalling

The Fig.1.7. shows a section, in which the depth is represented ( $AB = 566.3 \mu\text{m}$ ) and the length ( $CD = 342.4 \mu\text{m}$ ) (see Fig.1.7.). Still, in this case the  $CD$  length is not the length of trace left by the fiber after concrete destruction. To calculate the length of trace, the sinus function was applied (see Eq.(1.1)) for the inclination angle (See Fig.1.8.).

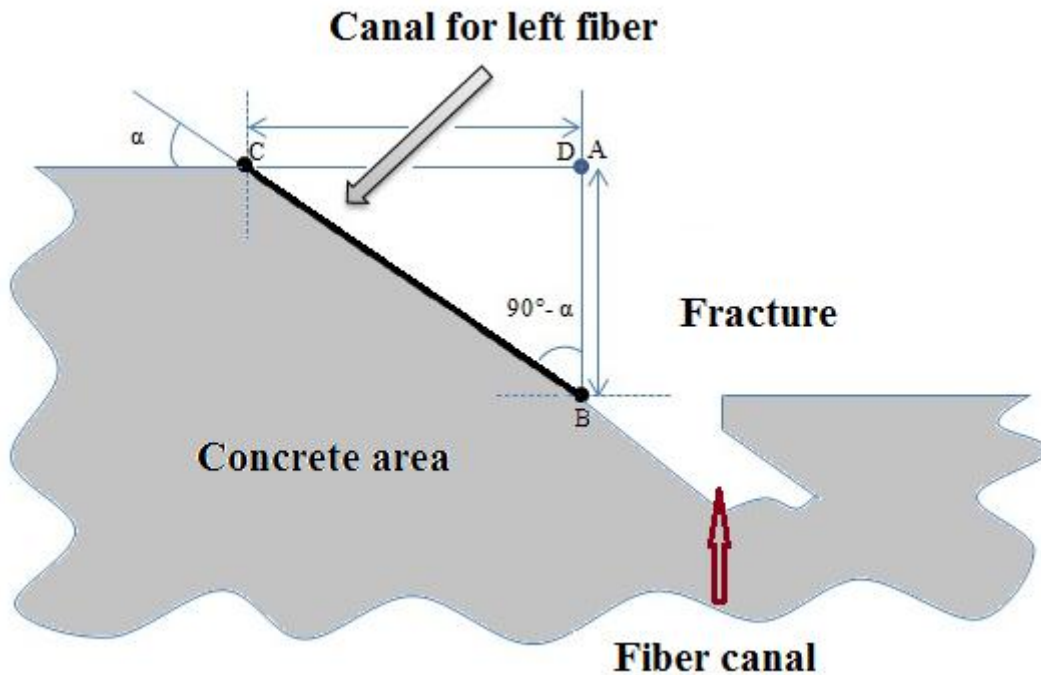


Fig.1.8. Canal surface when spalling the concrete and turning the fiber

$$\sin(90^\circ - \alpha) = \frac{CD}{CB} \quad (1.1)$$

where  $\alpha$  – fiber angle, °;

$CD$  – length obtained during experiments,  $\mu\text{m}$ ;

$CB$  – canal length left by the fiber when matrix is broken,  $\mu\text{m}$ .

Hence a formula (1.2) arises:

$$CB = \frac{CD}{\sin(90^\circ - \alpha)} \quad (1.2)$$

The point  $C$  in the Fig.1.6 is located higher than the studied length of trace  $\approx$  by 40% (diagram of Fig.1.6.). Hence  $CD = 342.4 \cdot (100\% - 40\%) = 342.4 \cdot 0.6 = 205.44 \mu\text{m}$  or  $0.205 \text{ mm}$ . We find  $CB$  by the formula (1.2):  $CB = 0.205 / \sin(90^\circ - 80^\circ) = 0.205 / \sin(10^\circ) = 0.205 / 0.1736 = 1.18 \text{ mm}$ . As the point  $D$  has been taken from the very beginning of the canal, the found distance  $1.18 \text{ mm}$  includes the diameter of the pull-out fiber and the length of the searched canal at concrete breaking. It is required from  $1.18 - (0.45 \div 0.5) - 0.1 = 0.58 \div 0.63 \text{ mm}$  – the true length left by the fiber after destruction of matrix.  $0.1 \text{ mm}$  – distance parting the fiber from the length of trace is left when the concrete matrix is damaged. The graph (see Fig.1.5) shows an intense decrease of the applied force to  $\approx 0.5 \div 0.6 \text{ mm}$ , which matches the found distance  $CB = 0.58 \div 0.63 \text{ mm}$ . Conclusion: the initial decrease is explained by the destruction of matrix of the sample tested by fiber. After matrix destruction the fiber has intense delaminating and pull-out of fiber of the concrete matrix by friction.

The Fig.1.9 shows the studied surface, where the fiber takes the maximum, intense surface deterioration when pull-out the fiber of the concrete matrix. It should be noted: a) surface is rugged with cavern formation; b) the surface has visible particles, which leads to friction and accumulation, and when pull-out the fiber to congestions. The diagram in fig.1.5 – with the length of 5.7 mm and 7.3 mm of the pull-out fiber we see the decline of force caused by congestions.



Fig.1.9. Canal surface left by the orientated fiber at an angle of 80°

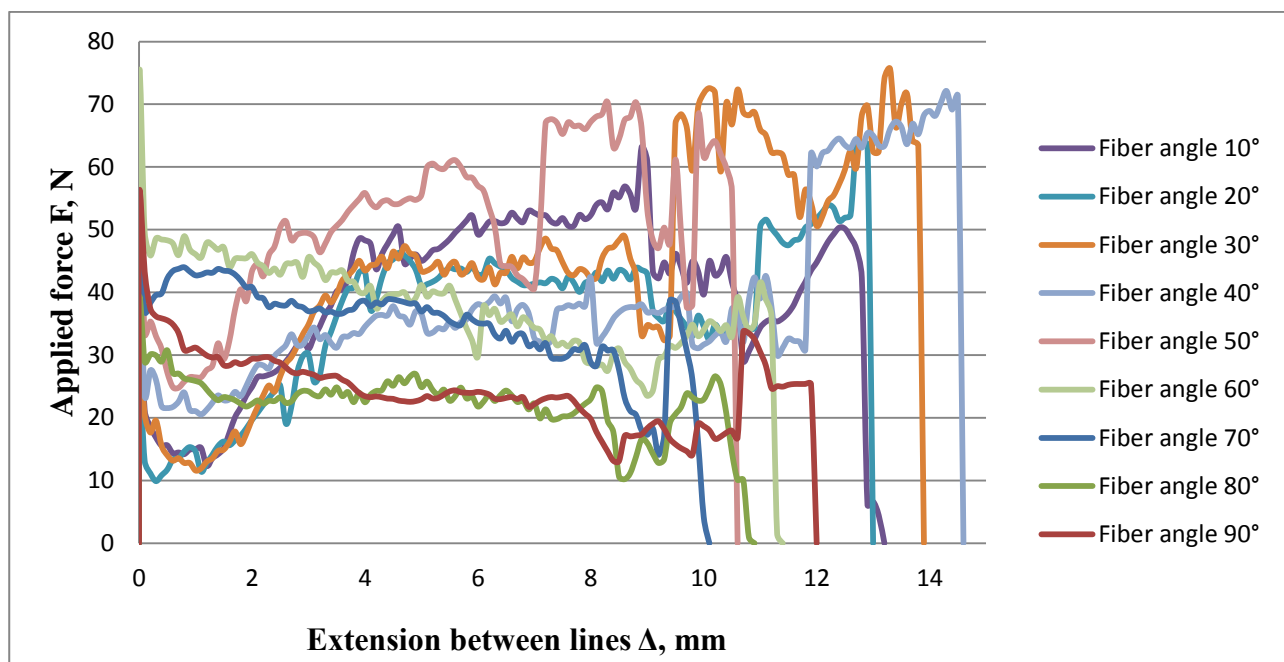


Fig.1.10. Average value of pull-out of one SSF of the concrete matrix at different angles inclination

The Fig.1.10. shows the initial force decline for all samples. The length, at which the pull-out fiber bears the load at the angles of  $50^{\circ}$ - $90^{\circ} = \approx 10 \div 12$  mm, and for samples at the angles of  $10^{\circ}$  -  $40^{\circ}$  is: length =  $\approx 13 - 14.7$  mm, and it is by  $8\% \div 32\%$  higher than at the angles of  $50^{\circ}$  -  $90^{\circ}$ . The explanation of this phenomenon – presence of large areas of concrete spalling on the places of fiber output of the matrix in both parts of the concrete sample.

**The third chapter** describes experimental results on deflection of fiberconcrete prisms bending. Prisms were tested for 4-point bending. Under applied external forced increase in the prism's, crosssection appeared – a main crack, the openings of which were followed depending on the value of the applied load. The prisms containing various concentrations of fibers with different geometry which were dispersed in the material's volume were studied. The results of the bearing capacity of prisms containing chaotically distributed fibers in the volume were compared to the result of the bearing capacity of prisms having layered structure. Besides, the layer geometry and percentage of fibers in them changed. Then is the chapter presents the results of the performed X-ray analysis for fiberconcrete prisms. The “weak” areas were found out (areas in material containing decreased fiber concentration and oriented unfavorably (perpendicularly to the beam's longitudinal axis)). This chapter gives the results of the performed experiments for bending of fiberconcrete prisms containing polymeric fibers. The results were analyzed and the maps of fiber arrangement on the crack's surface were received. Experimentally the inclination angles of each fiber towards the crack's surface were measured and the diagrams were built.

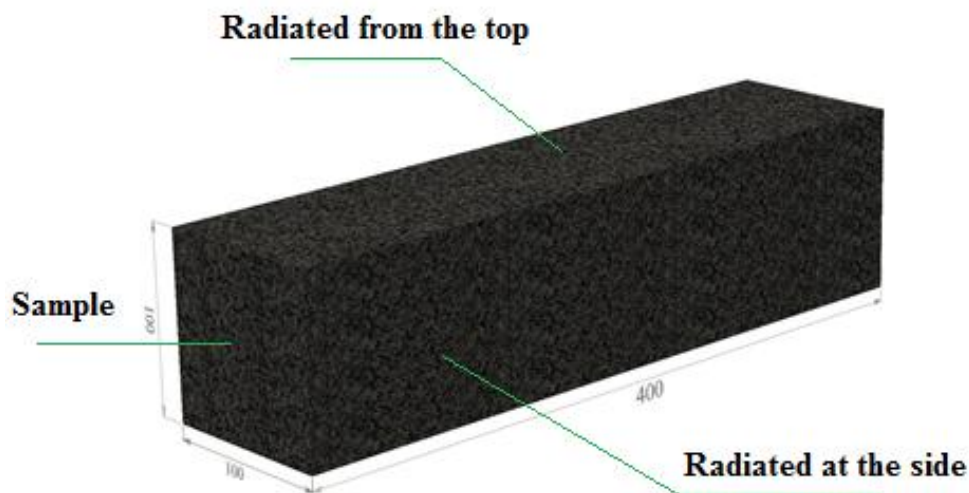


Fig.1.11. X-ray screening scheme for fiberconcrete

The Fig.1.11. represents schematically the X-raying procedure. The X-raying of samples was performed along two edges (X-raying was done from the top and at the side, Fig.1.11.).

Averagely 10 minutes are spent for each X-rayed frame of roentgen film, brand D7 Pb.

Having considered the x-ray image of the layered sample K2 –Fig.1.13., the crack will appear in the given place due to the least number of fibers incidence, which are located not vertically to the main surface of the crack. The x-ray images of layered fiberconcrete point to the fact that attempts to orientate fibers in the samples with the help of combs failed.

X-ray pictures of layered fiberconcrete [7]:



Fig.1.12. X-ray image of fiberconcrete K2 (screened from the top)



Fig.1.13. X-ray image of fiberconcrete K2 (screened at the side)

Results with 4 point bending

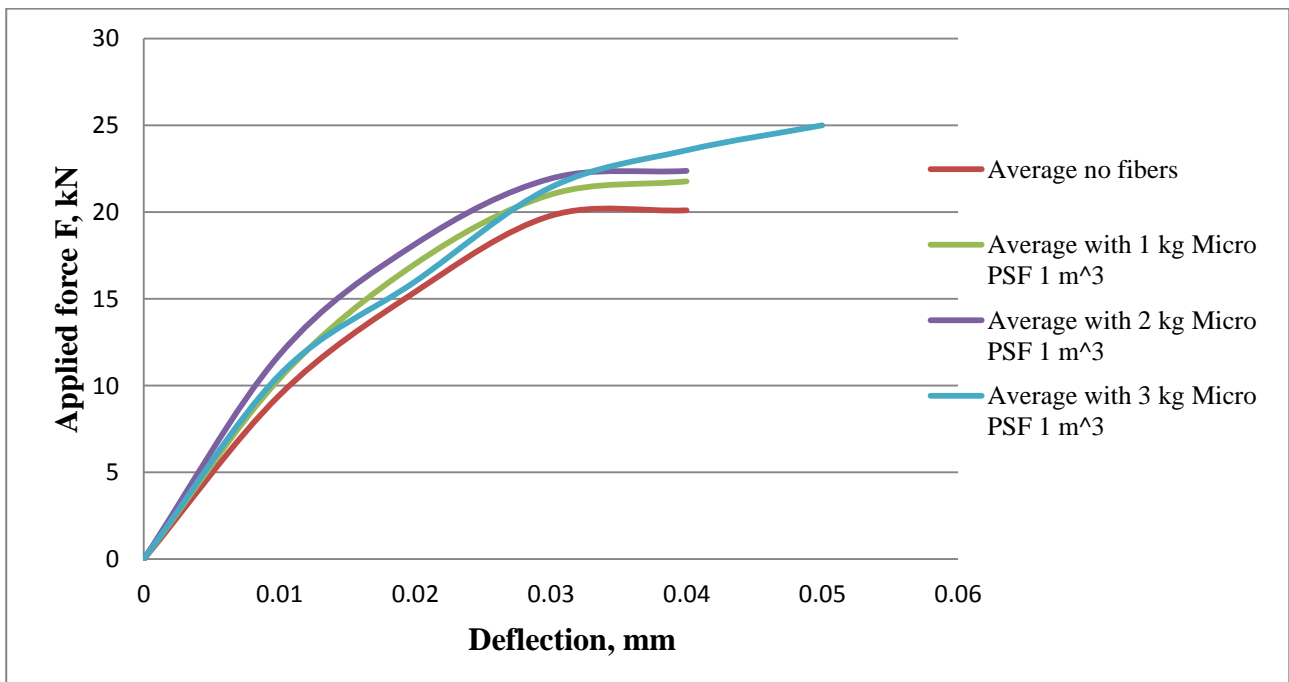


Fig.1.14. Averaged curves “force – vertical displacement of the middle of fiberconcrete prism” with micro PSF tested for 4-point bending

Due to uneven vibration on the vibration exciter the vibration loops appeared, which, in their turn, turned one edge of the fiber and down the fiber into the bottom of the concrete matrix. It should be taken into consideration that the resistance of concrete and drowning of fibers is different, thereby fibers gradually sink into the bottom of matrix when there is oscillation [15].

The diagrams of force – bending of the middle point of prism with 4-point bending were received. The Fig.1.14. shows how the applied force and the bending of the middle point of fiberconcrete prism increase depending on the increase of number of micro PSF per  $1\text{m}^3$ . The samples containing micro PSF in the amount of  $3\text{ kg/m}^3$  bear large load (fibers bear the applied force) with larger bending (which was equal to  $\approx 0.052\text{ mm}$ ).

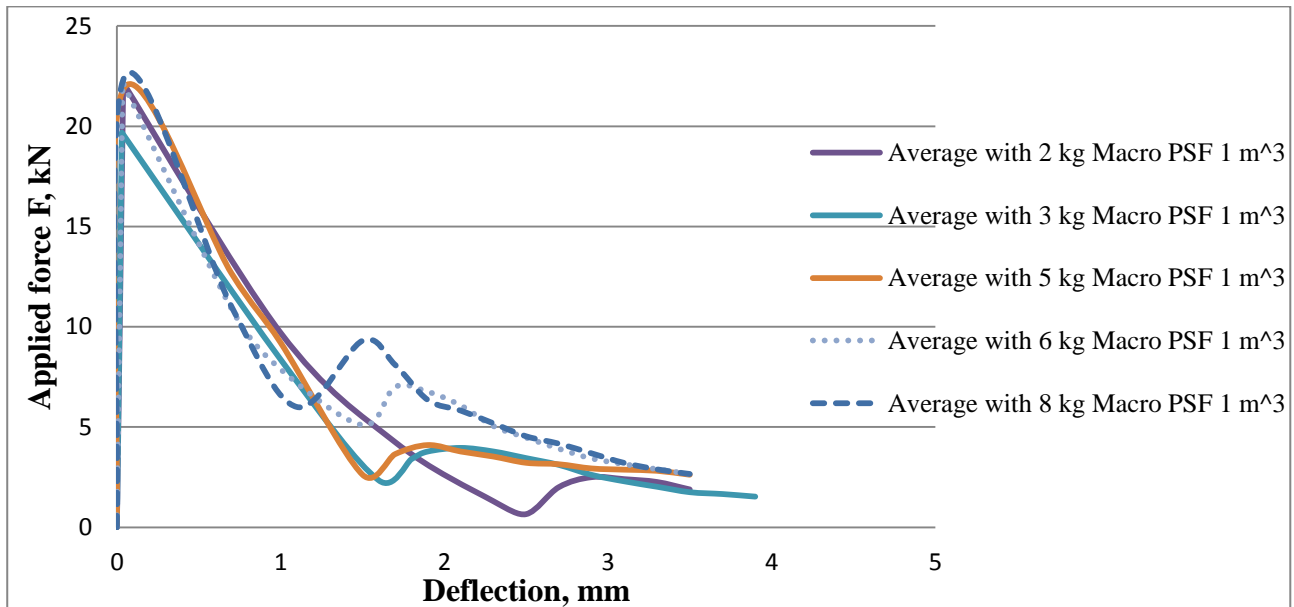


Fig.1.15. Average values of “force – vertical bending of the middle of fiberconcrete prism for fiberconcrete with macro PSF after testing for 4-point bending

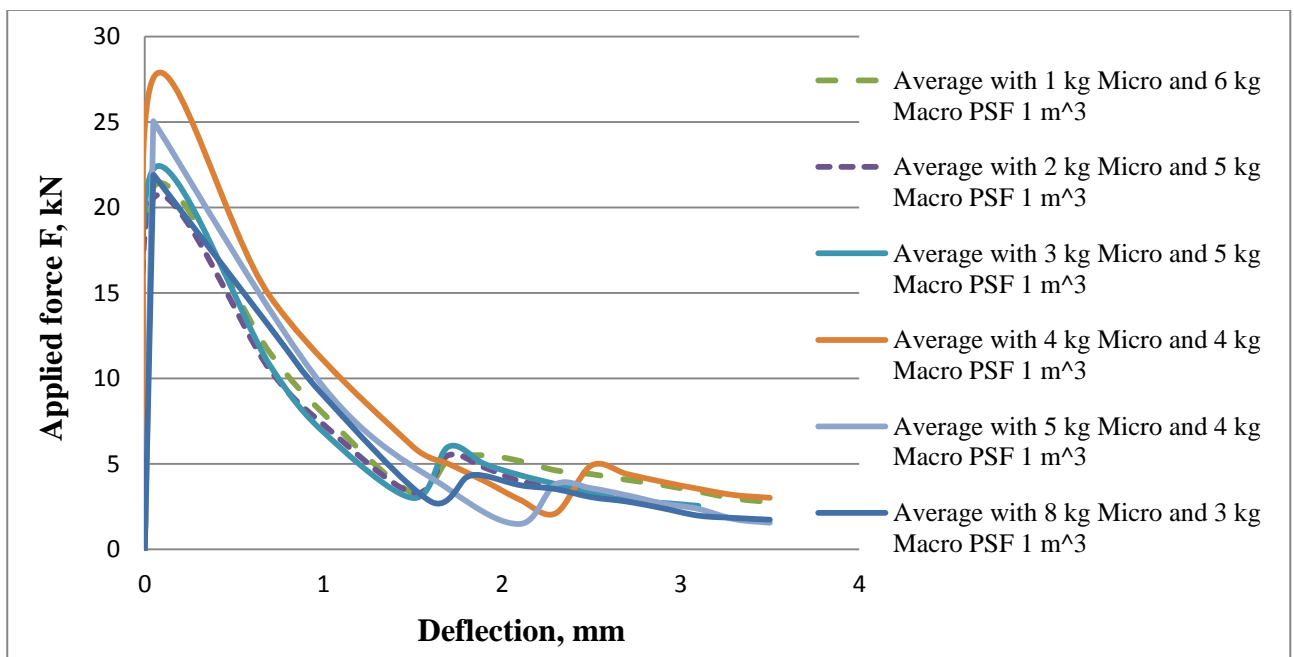


Fig.1.16. Average values of fiberconcrete with micro and macro PSF after testing for 4-point bending

As the micro PSF is relatively short and has small diameter, then the amount of such fibers in the material is considerably higher if comparing to the concrete containing the same amount of kilos of macro PSF. However, the lengths of pill-out ends of fibers during break-up for micro PSF are shorter than those for macro PSF. The break-up takes place quasi fragile, the permitted opening of the crack (where the fibers bear the whole load) is very small (see Fig.1.14.) [1]

Inspection (using a microscope) of surface of the opened crack shows the location of micro PSF in the main crack. The fibers are located rather chaotically along the whole surface with low degree of bunching.

The Fig.1.15. shows the obtained experimental data (in tests for 4-point bending) for fiberconcrete containing macro PSF. 2 stages can be distinguished on the curves. Stage 1 – fiberconcrete at the stage of crack opening shows sharp decrease of the bearing capacity; this is explained by the fact that flexibility module of macro synthetic fibers is small and only a part of fibers is loaded in the crack. Stage 2 – repeated increase of the bearing capacity can be explained by the fact that macro PSF stop delaminating and transfer [11] to the mode of flexible plastic deformation of the fibers themselves, bearing the largest loads.

The Fig.1.16. shows the diagrams of experimental data of this fiberconcrete with fiber-cocktails of micro and macro PSF tested for 4-point bending. Adding micro and macro synthetic fibers to the concrete we observe increase of the bearing capacity of fiberconcrete, increase of strength, as well as presence of Stage 2 demolition, like on the previously considered diagrams of Fig.1.15.

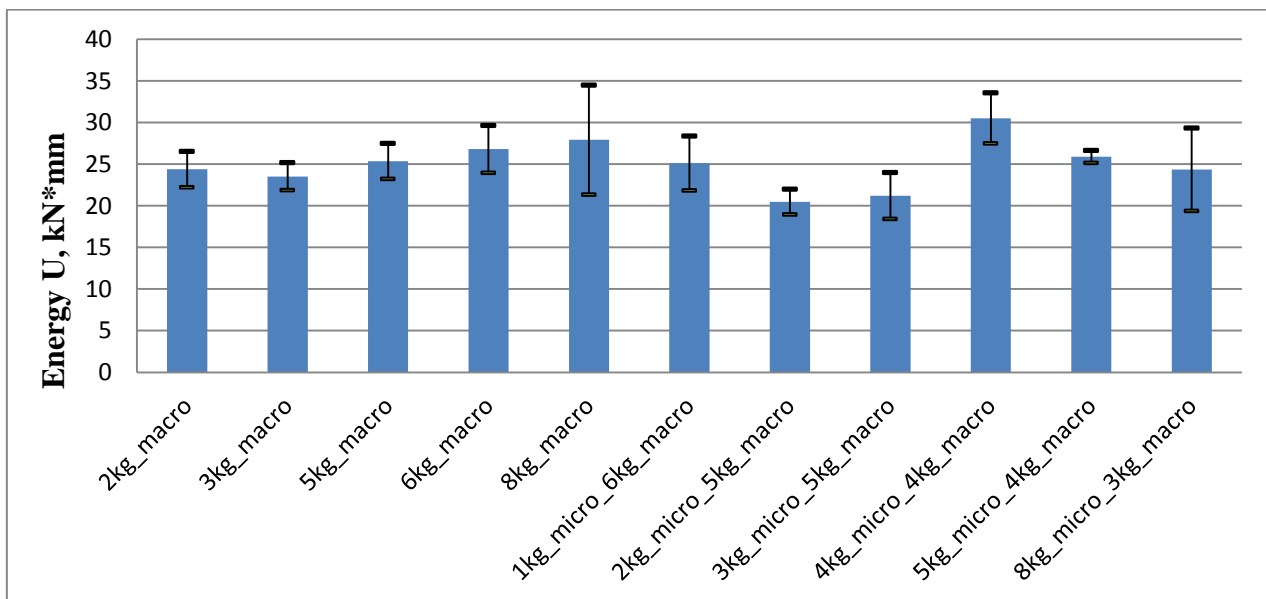


Fig.1.17. Average value of spent energy for bending, and the crack opening of beams with macro PSF and fiber-cocktails of micro with macro PSF

It is seen from the data of Fig.1.17. that increasing the concentration of macro PSF [6] in the concrete the energy spent for bending is increased, as well as the crack opening. The samples with 2 kg of macro PSF has the following average energy for bending =  $\approx 24.4$  kN\*mm, which is by  $\approx 13\%$  less than for samples with  $8 \text{ kg/m}^3$  [2]

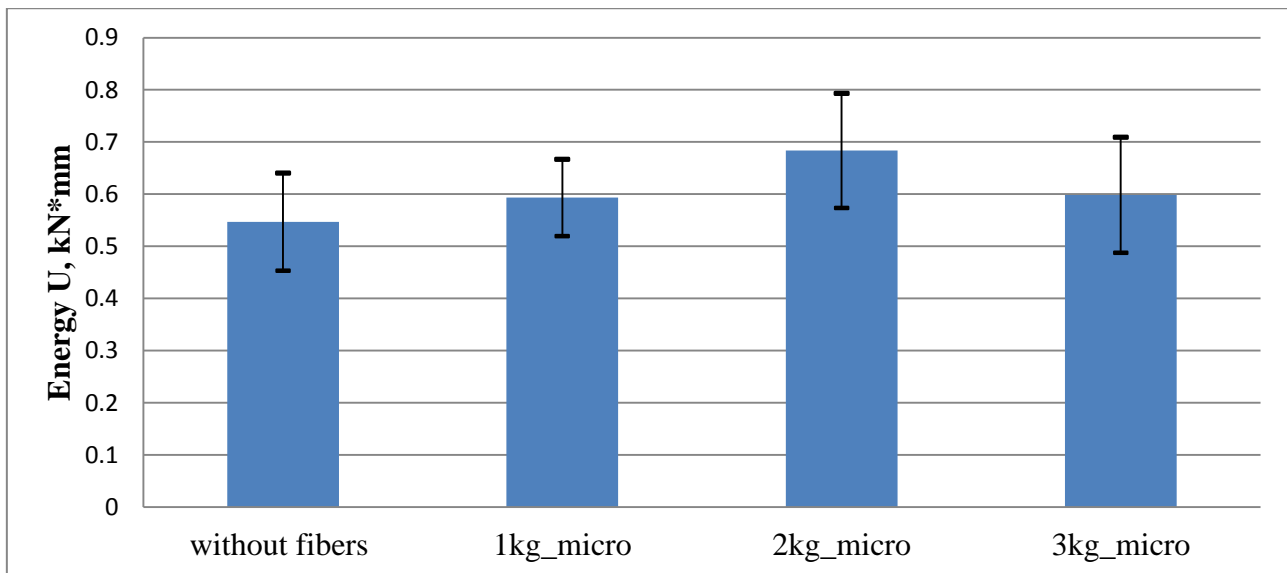


Fig.1.18. Average values of spent energy for bending, and opening of crack of beams with micro PSF

Micro PSF, when mixing with macro PSF, facilitate necking of macro fiber by the concrete (concrete + micro fiber) during its pull-out at the initial stage of crack opening and cannot equally replace the macro PSF (as the bearing capacity of the beam containing microfibers ends with kinks (approximately equal to crack opening) and equal to 0,04mm). Let us take 3 kg of macro, which has the average energy =  $\approx 23.5$  kN\*mm, which is by  $\approx 4$  % less than comparing to cocktails of 8 kg micro and 3 kg macro. Of course, the samples with  $8 \text{ kg/m}^3$  macro bear the highest load of all obtained data, Fig.1.17.

It arises from the diagrams (see Fig.1.19.) that with small concentration of fibers the fiberconcrete with homogeneous distribution of fibers (fibers are located chaotically along the volume) bears both the least peak load, comparing to the layered samples (fibers are located only in the specific layer of concrete), and shows the least bearing capacity along all opening of main crack. It arises that during formation of fiberconcrete in layers, we can reach large bending strength. A conclusion is ready of comparison of average values of the obtained layered fiberconcrete (see Fig.1.19.): selection of location of the layer level influences the bearing capacity, i.e., for layered samples  $50 \times 25 \times 25$  mm the obtained average value for deflection is higher than for  $25 \times 50 \times 25$  mm. According to Fig.1.21., the average energy for samples  $50 \times 25 \times 25$  mm reaches  $\approx 78$  kN\*mm, and for the sample  $25 \times 50 \times 25$  mm  $\approx 63$  kN\*mm, which is by  $\approx 19$  % less than comparing to the samples having configuration of  $50 \times 25 \times 25$  mm. It is important also to know, at which exploitation loads it is planned to use plates or beams, which model the tested sample data. In case of one-sided deflection it is obvious that reinforcement [17] of the lower sample layer leads to large increase of the bearing capacity than reinforcement of the lower and the upper layer simultaneously. The upper layer, during deflection, is subject to compressing load [13] and partially the tensile load (neutral line goes through the layer), thereby its contribution to the beam's bearing capacity is limited, because the tensile load prevails in the lower layer [3], and the concentration of fibers in it is small. The average obtained energy for deflection for homogeneous fiberconcrete is equal to  $\approx 51$  kN\*mm, which is by  $\approx 19\%$  less than for orientated layered fiberconcrete  $25 \times 50 \times 25$  mm, and by  $\approx 35\%$  less than for layered fiberconcrete  $50 \times 25 \times 25$  mm.

Tested for four-point bending with SSF that are 26 mm long and have diameter of  $0.45 \pm 0.5$  mm.

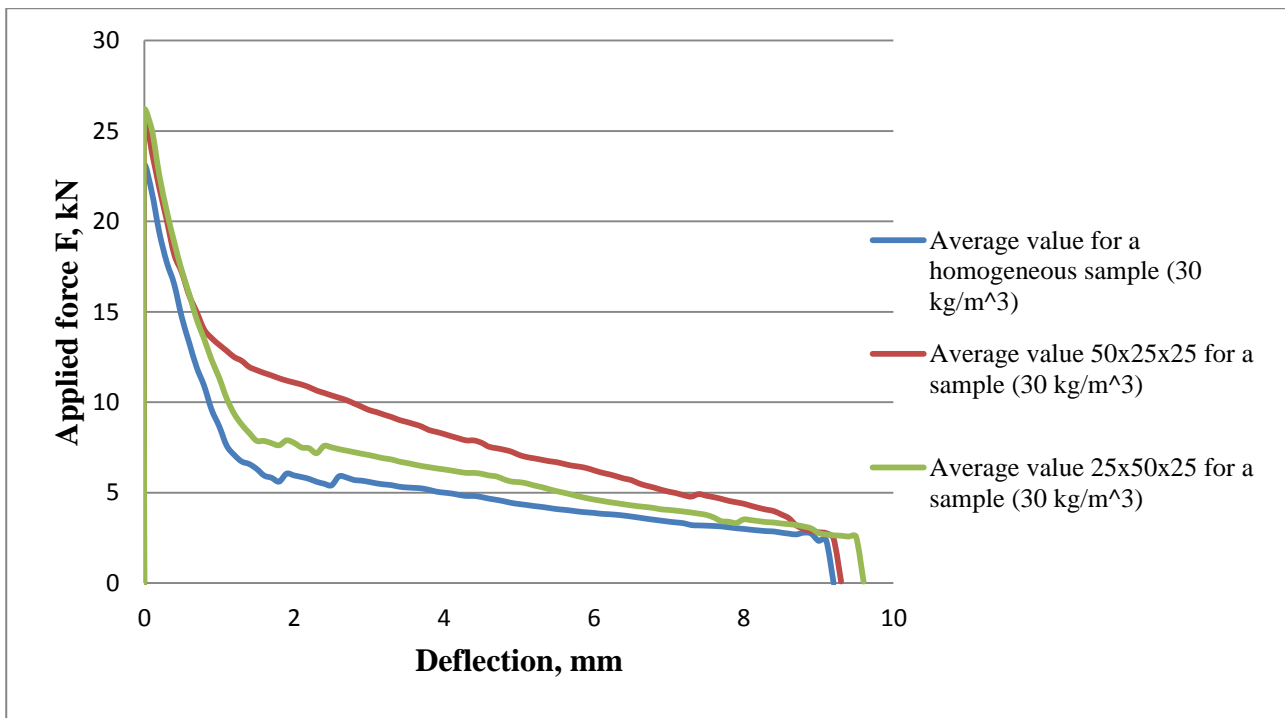


Fig.1.19. Curves of average values of bending of the middle of prism depending on the applied bending load of homogeneous and layered fiberconcrete with the total (per whole sample) concentration of fibers  $30 \text{ kg/m}^3$

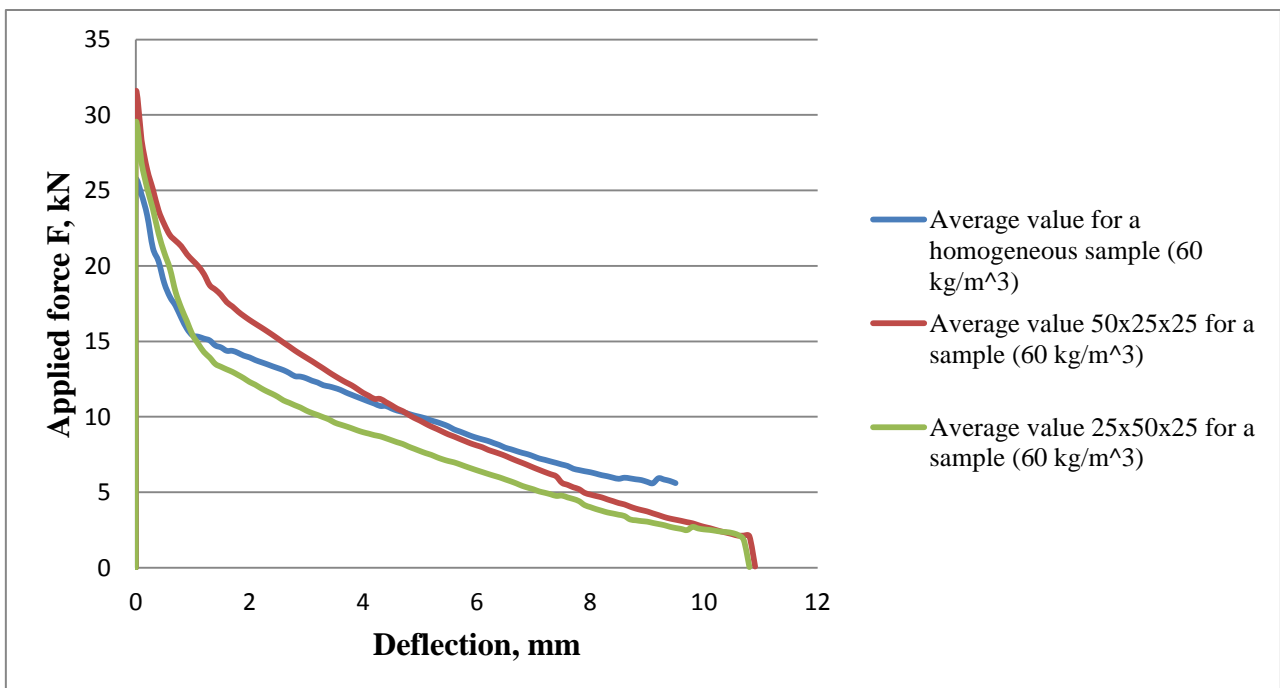


Fig.1.20. Curves of average values of deflection of the middle of prism depending on the applied bending load of homogeneous and layered fiberconcrete with the total (per whole sample) concentration of fibers  $60 \text{ kg/m}^3$

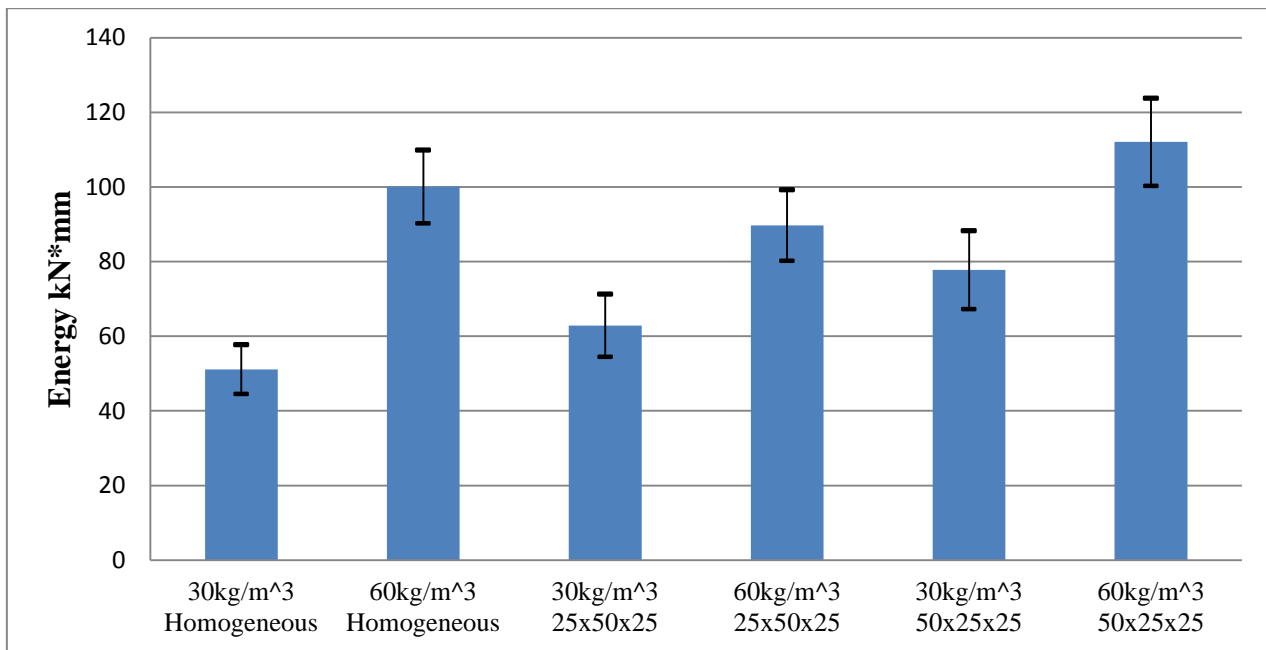


Fig.1.21. Average value of spent deflection energy with SSF that are 26 mm long and have diameter of 0.45÷0.5 mm

The Fig.1.21. – by increase of concentration of fibers the averaged curves behave differently. Prisms of homogeneous fiberconcrete at deflection, when increasing the concentration of fibers by  $m^3$ , managed to bear the least load with the maximum crack  $\approx 1$  mm. After reaching the crack opening of 1 mm, the value of the required applied force grows, if comparing to the layered samples 25x50x25 mm, which is caused by the fact that in the homogeneous samples, during the procedure of bearing the external load, the fibers connect, which are located higher and higher along the beam section. This phenomenon proves again that the upper layer at deflection takes less part in the bearing capacity (does not work for pull-out) of the beam [4]. Comparing homogeneous and layered beams, it is clear that homogeneous fiberconcrete bears less deflection force to the beam deflection that is equal to  $\approx 4.6$  mm, after this, it has higher bearing capacity to 9.5 mm. With the following increase of concentration of fibers per  $m^3$  a moment comes when the fiberconcrete layers will have that much fiber that the load-bearing mechanism in the section by pull-out individual fibers will start changing to the load-bearing mechanism in the section by pull-out concrete fiber blocks, which might lead to reverse action: layered fiberconcrete will bear the least applied force. It is clear from Fig.1.21, that the average energy for homogeneous fiberconcrete with concentration of fibers  $60 \text{ kg/m}^3 \approx 100 \text{ kN*mm}$ , and for the layered 25x50x25 mm with concentration  $60 \text{ kg/m}^3 \approx 90 \text{ kN*mm}$ , which is by 10% less than for the homogeneous. Energy of layered fiberconcrete 50x25x25 mm with  $60 \text{ kg/m}^3 \approx 112 \text{ kN*mm}$ , it is by  $\approx 20\%$  more than for 25x50x25 mm and by  $\approx 11\%$  - than for the homogeneous.

**Chapter 4** presents the results of numerical modeling for mould filling by a fiberconcrete mix. Special attention is paid to identification of areas with high vertical speed component [10] gradient. It is assumed that the mentioned areas will lead to increased concentration of unfavorably oriented fibers (due to acting shear flow perpendicularly to the beam's axis [16]) in the beam's crosssections.

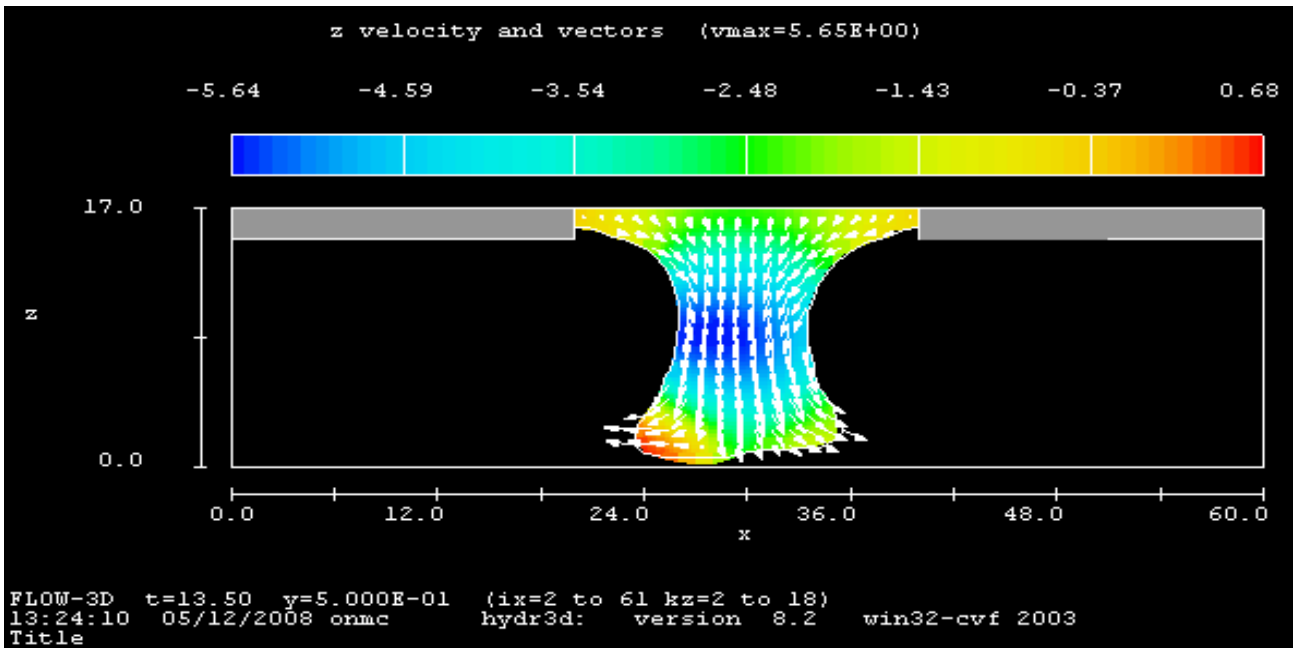


Fig.1.22. Fiberconcrete fluid flowing at t=13.5 s

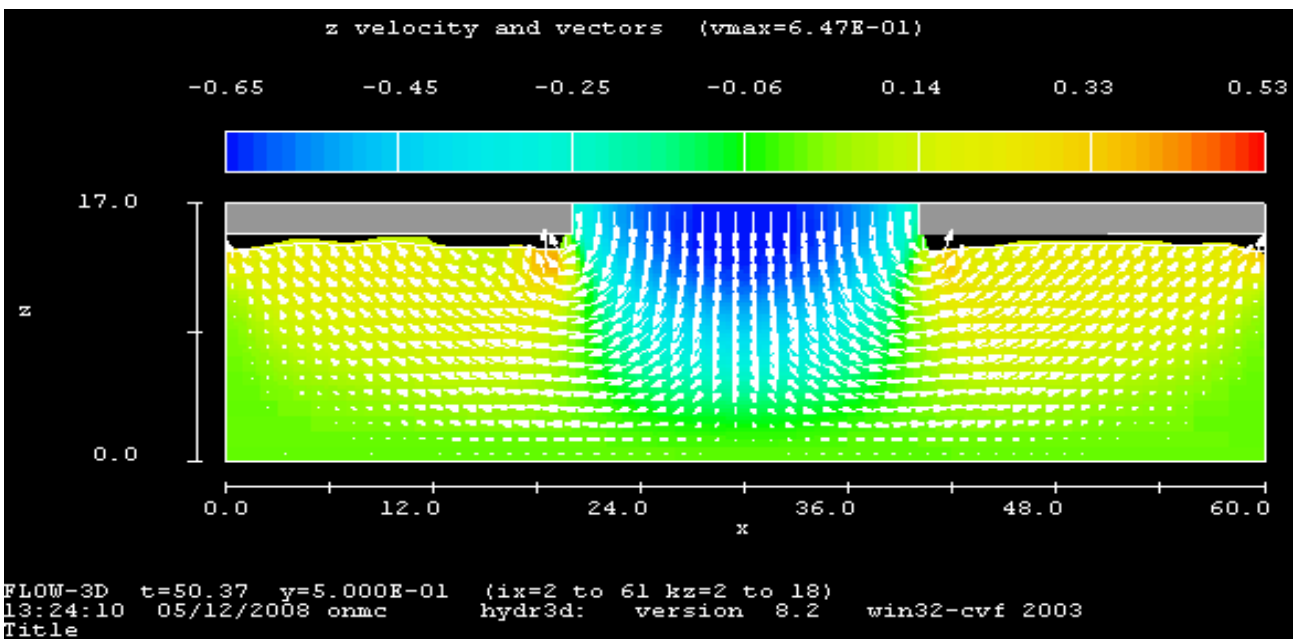


Fig.1.23. Mould with dimensions of 60x15x15 is filled with viscous fluid

Fig.1.23.shows that within time  $t=50.37s$ , the fluid fills in the mould. There is a space between the fluid and the mould's cover, it can be explained as there is pressure (1 atmosphere), which hereby does not allow the fluid filling all capacity. The arrows in the Fig.1.23 point to the direction of viscous fluid's speed vector [5].

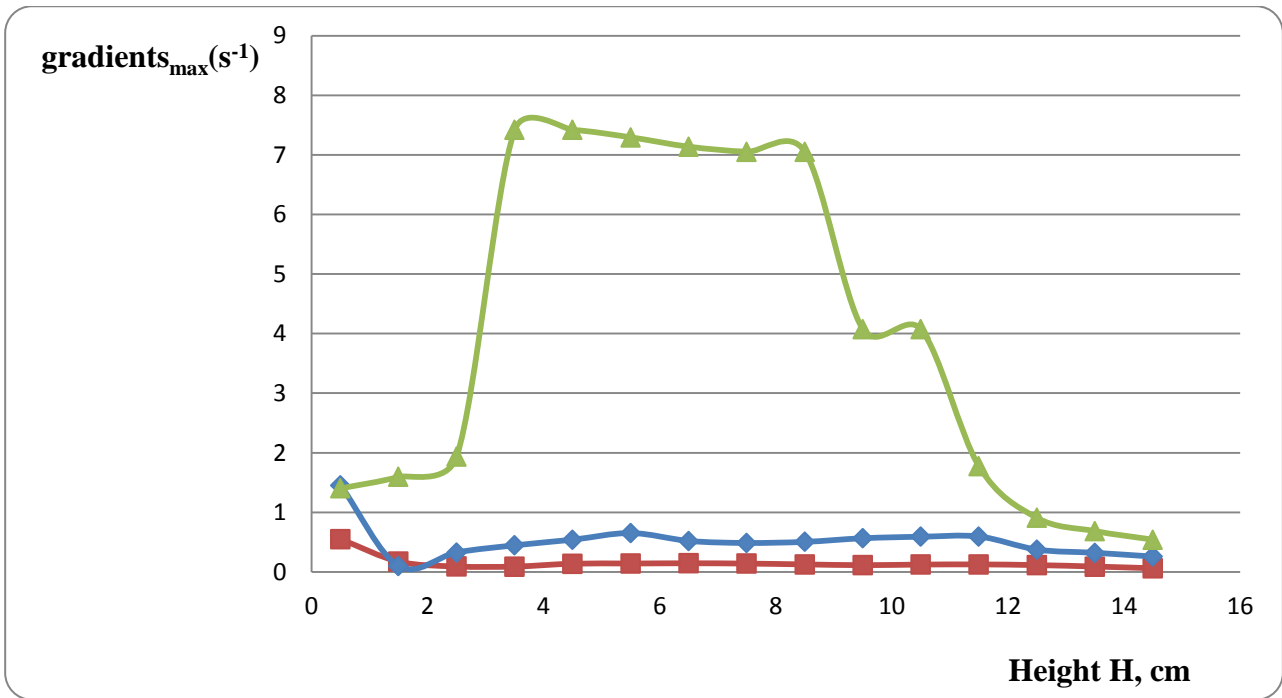


Fig.1.24. Maximum gradient image by the absolute value, where ■ at  $Vz_n=29.5$  cm and  $Vz_{n+1}=31.5$  cm ◆ at  $Vz_n=32.5$  cm and  $Vz_{n+1}=33.5$  cm ▲ at  $Vz_n=35.5$  cm and  $Vz_{n+1}=36.5$  cm

It follows from the Fig.1.24. that at  $Vz_n = 35.5$  cm and  $Vz_{n+1} = 36.5$  cm there is the largest fiber vertical turning possibility of three considered verticals. It is explained the following way: pouring fluid the fibers (at  $Vz_n=35.5$  cm and  $Vz_{n+1}=36.5$  cm) are located farther from the flow center and turn more often than the fibers, which are located closer to the fluid flow center. There, where the  $\text{gradient}_{\max}$  is larger, is larger possibility that there will be vertically orientated fibers, which are decreasing fiberconcrete prism bending strength. At  $Vz_n=29.5$  cm and  $Vz_{n+1}=31.5$  cm, the fibers practically do not turn around, because the maximum gradients are small comparing to two other cases, and the considered flow is located in all fluid flow center. Regarding the three considered verticals we can conclude that at the height from 0 cm to 5 cm it is less possible that the fibers will turn vertically, because the fibers touch the mould's bottom and herewith fiber vertical turning is impossible. At the height from 5 cm to 11 cm, we observe the largest possibility that the fibers will turn vertically, as there is no contact with the mould and there is the highest flow speed, which hereby attempts to straighten the fibers vertically. At the height from 11 cm to 15 cm, it is less possible that the fibers will turn vertically, because the fluid is poured into the mould and it cannot manage to level vertically within a short period of time, unless the fiber is not located vertically immediately or located in a wide angle against the mould's lower surface.

Conclusion: filling the moulds with fiberconcrete, pouring it vertically in the mould's middle area, zones with undesired fiber orientation are formed with large possibility in the prism's middle part (fibers turn perpendicularly to the prism's longitudinal axis, decreasing the given split's bearing capacity). In these zones, fiber orientation cannot be considered chaotic.

**The Chapter 5** describes the algorithms of 4 numerical models are predicting the fiberconcrete beam's bearing capacity under the bending load. Predictions correspond to the stage of macrocrack opening and fiber pull-out from its flanks. Data on mechanics of a single fiber pull-out from the crack's flanks in the concrete are taken out of the previous chapters.

Model 1 – assumes that all fibers are located in the volume chaotically.

Model 2 – uses experimental data on fibers location on the crack’s flanks and their orientation.

Model 3 – arises from the assumption that all fibers are crossing the crack are located strictly perpendicularly to it’s plane.

Model 4 – is used for description of the bearing capacity of layered fiberconcrete beams with different concentration of fibers in the samples.

The following curves with PSF, 30 mm length and 0.55 mm diameter, were received. In the model 1 the curves of average values of deflection of the prism’s middle are presented depending on the applied bending load (each curve was received by data averaging by 10 samples with each fiber concentration per 1 m<sup>3</sup>).

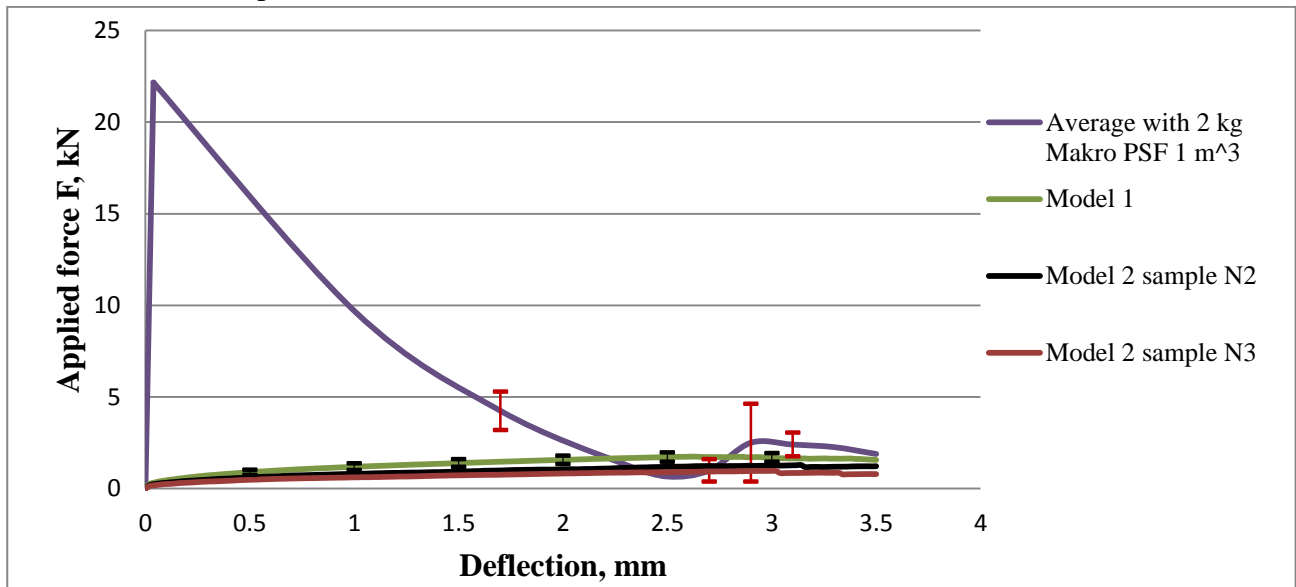


Fig.1.25. Averaged curves “force – vertical deflection” for homogeneous fiberconcrete with macro fiber concentration 2 kg/m<sup>3</sup> after testing for 4-point bending and modelling

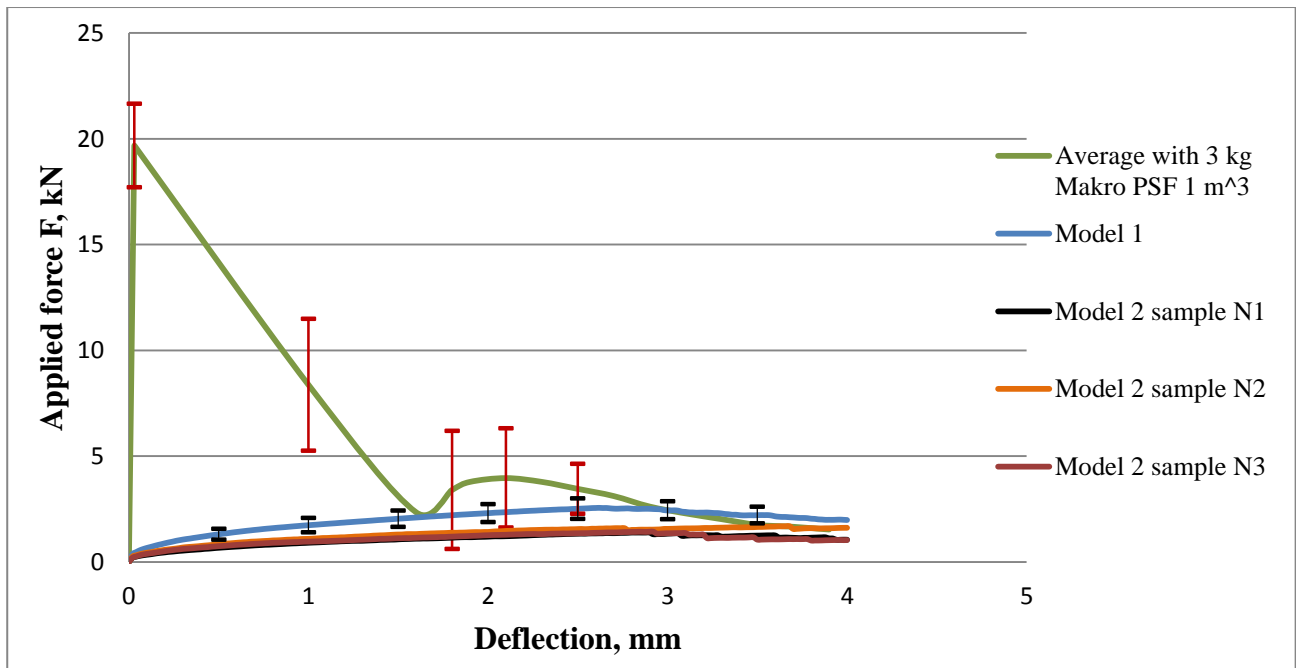


Fig.1.26. Averaged curves “force – vertical deflection” for homogeneous fiberconcrete with macro fiber concentration 3 kg/m<sup>3</sup> after testing for 4-point bending and modelling

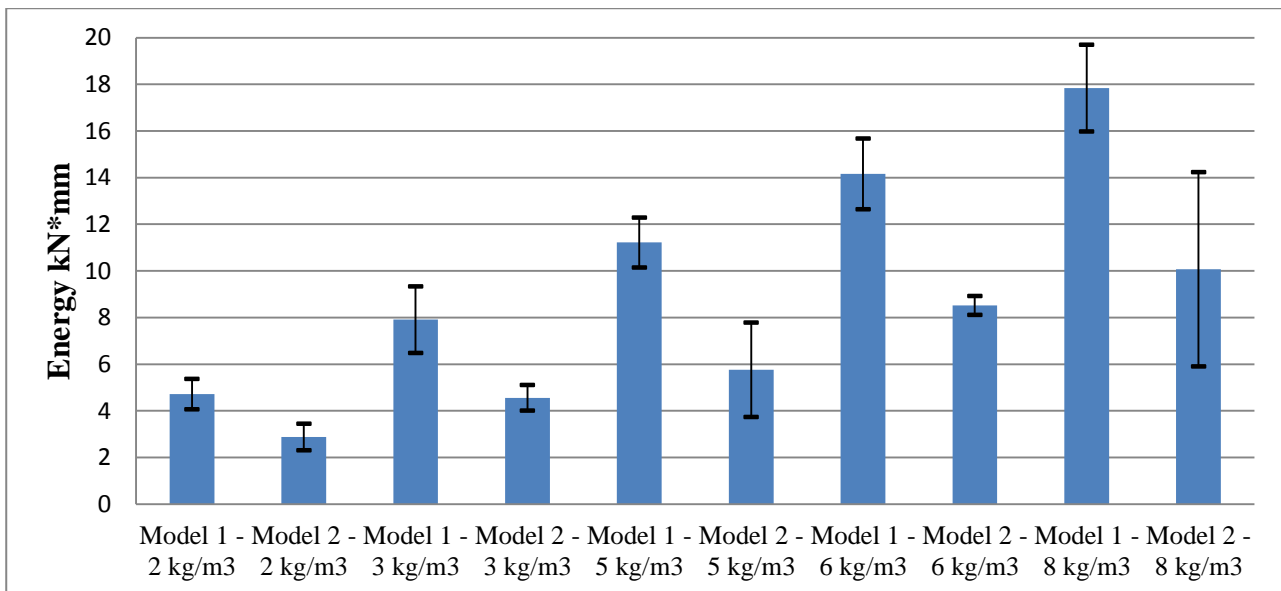


Fig.1.27. Energy of fiber work for 4-point bending - taking only the plastic deformations and fiber frictions into account

Let us consider the curves “force–crack opening at prism deflection with polymeric synthetic fibers (see Fig.1.25. – 1.26.). Models 1 and 2 are not description of the received experimental data, as the given models contain a limited number of micro mechanisms, which, in their turn, show the border between the reality and the modeling. Experimental data contain such micro mechanisms like: work for crack opening in the concrete, work for fiber loading at the initial stage of crack opening, work for plastic deformation and friction, work for fiber rupture.

Model 1 takes into account the following:

- a) imitates accidental fiber position in the material’s volume and respectively in the crack;
- b) stochastically even (averagely) fiber arrangement by the whole volume, both by inclination angles and pull-out lengths.

Model 2 takes into account the following:

- a) real amount of fibers in the crack (calculated after sample fracture);
- b) real location of fibers on the crack’s surface and location of each fiber by the length ( $y$ );
- c) the smallest angle to the crack’s surface ( $\alpha$ ).

Comparing the two models, the bearing load of the first model is bigger because the fibers are located evenly and the number of estimated fibers is bigger than in the model, in which the real number of fibers and chaotic arrangement is taken into account. Uneven arrangement is caused by the fact that the current layer is thin (relation of fiber’s length and sample’s height  $\approx 1$  to 3) and when pouring from the concrete mixer orientation and turning of fibers to the horizon is caused. Less is given by the specific realization with heterogeneity of arrangement, and fiber orientation as a result of gradients of flowing rate (when filling the mould with fiberconcrete (pouring fiberconcrete from the top into the middle parts of the mould)) may be positioned lower (giving much lower bearing capacity of the prism during the deflection) due to appearance of “weak” sections in the prism). Weak section is described by a large amount of fibers orientated at the angles that are close to  $0^\circ$  due to big shearing deformations in the liquid fiberconcrete during pouring. In a weak section of the model 1, it is not formed with even and chaotic fiber dispersal by the coordinates and the angles in the prism’s volume. It shows that the bearing capacity is the least, which is absolutely unobvious.

The following curves with SSF, 26 mm long and with diameter of  $0.45 \div 0.5$  mm, were received [14]

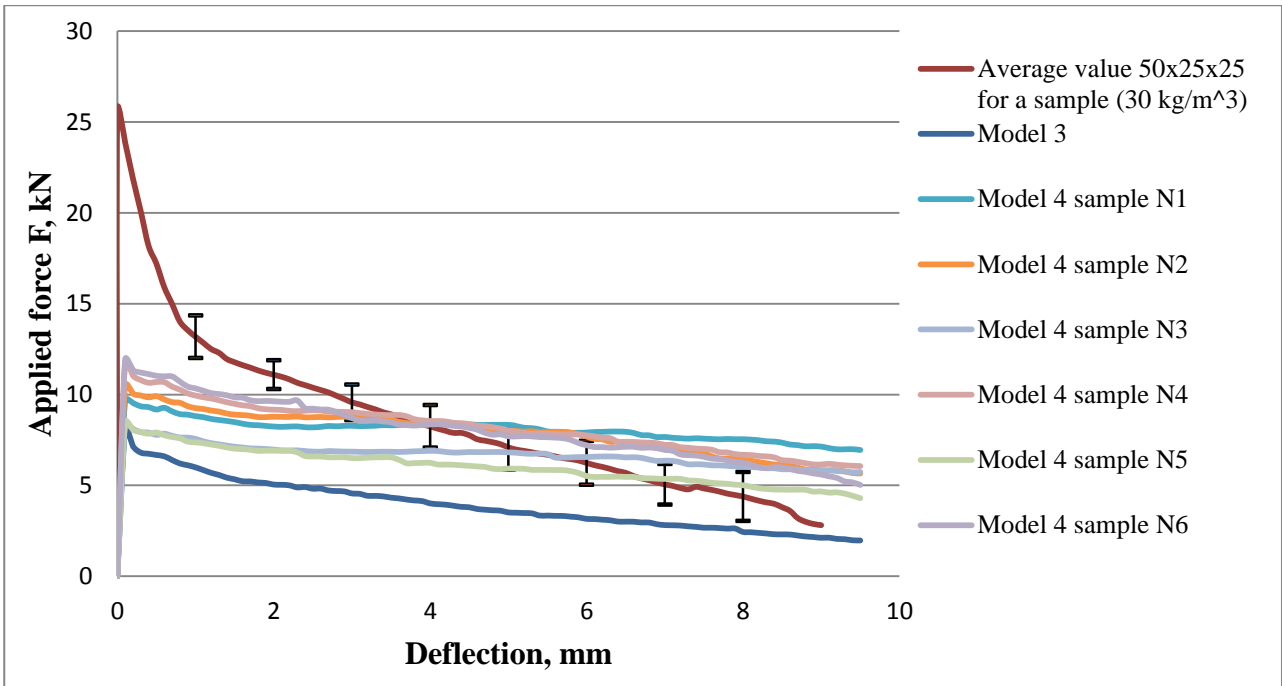


Fig.1.28. Averaged curves “force – vertical deflection for layered fiberconcrete with SSF concentration  $30 \text{ kg/m}^3$  after testing for 4-point bending and modelling

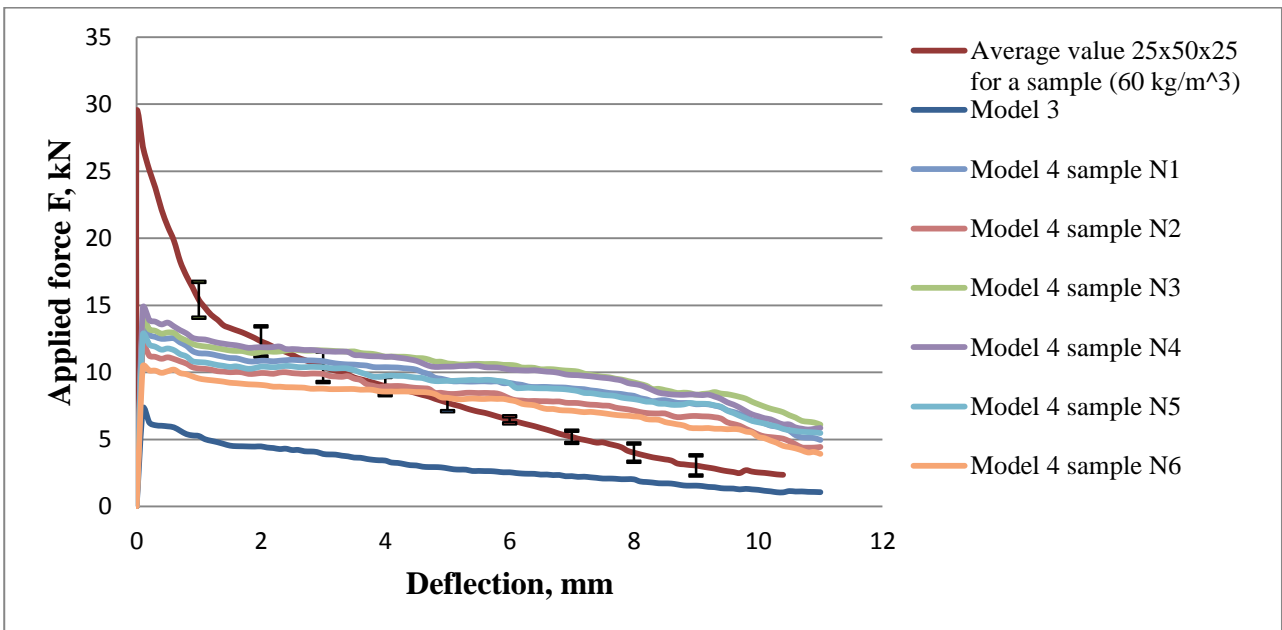


Fig.1.29. Averaged curves “force – vertical deflection for layered fiberconcrete with SSF concentration  $60 \text{ kg/m}^3$  after testing for 4-point bending and modelling

Theoretical and experimental data show that there is convergence of theoretical data with the confidence interval of experimental data. Theoretical data describe the performed work of the fiber at 4-point bending, it is seen that in the beginning of the diagrams the applied forces are increasing, and then the bearing capacity is decreasing after  $\approx 2.7 - 3$  mm of the main crack’s opening. Further

force application will lead to the moment when in this sample all fibers will be subject to rupture and the sample will break.

The Fig.1.27. presents the fibers' working energy for 4-point bending. By increase of fiber concentration the work get increased at 4-point bending. The samples with  $2\text{kg/m}^3$  have the energy of  $\approx 2.88 \text{ kN}\cdot\text{mm}$ , which is by 71% less than for the samples with  $8\text{kg/m}^3$ . Let us compare the average experimental data of energies with the received data of the Model 3:

- a)  $2\text{kg/m}^3$  average experimental data energy  $\approx 24.38 \text{ kN}\cdot\text{mm}$ , which is by  $\approx 88\%$  less than that for the theoretical.
- b)  $3\text{kg/m}^3$  average experimental data energy  $\approx 23.5 \text{ kN}\cdot\text{mm}$ , which is by  $\approx 80\%$  less than that for the theoretical.
- c)  $5\text{kg/m}^3$  average experimental data energy  $\approx 25.35 \text{ kN}\cdot\text{mm}$ , which is by  $\approx 77\%$  less than that for the theoretical.
- d)  $6\text{kg/m}^3$  average experimental data energy  $\approx 26.79 \text{ kN}\cdot\text{mm}$ , which is by  $\approx 68\%$  less than that for the theoretical.
- e)  $8\text{kg/m}^3$  average experimental data energy  $\approx 27.90 \text{ kN}\cdot\text{mm}$ , which is by  $\approx 64\%$  less than that for the theoretical.

It is seen from a-e that with increase of fiber concentration the fiber work gets increased and the work of other mechanisms not taken into account gets decreased.

With the crack opening of  $\approx 2.5 \text{ mm}$  we observe convergence of theoretical data with the average experimental data. Conclusion: with the help of the Models 1 and 2 we can foresee the bearing capacity the PSF, 30 mm length and diameter of 0.55 mm will have with deflection 2.5 – 4 mm and fiber concentration  $2 \text{ kg/m}^3$ ,  $3 \text{ kg/m}^3$ ,  $5 \text{ kg/m}^3$ ,  $6 \text{ kg/m}^3$ ,  $8 \text{ kg/m}^3$ .

The experimental and theoretical data of layered fiberconcrete have been considered in Fig.1.28. – 1.29., with concentration of SSF  $30 \text{ kg/m}^3$  and  $60 \text{ kg/m}^3$ . Model 3 shows on the images the least anticipated bearing capacity of fiberconcrete, if comparing to the model 4. Comparing with experimental data of the model 3, we can see that there is only approximation to the experimental data along all crack opening. This is caused by the fact that in the model 3 the bearing capacity of pull-out fibers located perpendicularly to the crack's surface is smaller (at  $90^\circ$  in pull-out) than for the fibers located at the angles from  $10$  to  $50^\circ$ . The prediction of the model using a hypothesis that all fibers in the crack's section are perpendicular to its banks gives much lower bearing capacity, see value Model 3.

Model 4 describes the fiber behavior in the crack taking the inclination angle ( $\alpha$ ), fiber height ( $y$ ), as well as length of pull-out fiber ( $c$ ), into account. Model 4 and experimental data are closer to each other than the model 3. This is connected with the fact that the experimentally received data of fiber orientation in the main crack approach the real (true) data. Conclusion: with the help of models 3 and 4 we can predict the bearing capacity the straight steel fibers, 26 mm long and with diameter of 0.45, will have at the deflection from  $\approx 1.5 \text{ mm}$  (depending on the fiber concentration). To maximally approach the experimental (true) data, it is required to analyze the performance of mechanisms not included in the models (work for crack opening in concrete, work for fiber loading at the initial stage of crack opening, work for fiber pull-out (in the model, it is partially taken into account, the behavior of fibers, which were pull-out from the concrete at the length that was bigger than a half of the fiber itself, is not taken into account)).

## CONCLUSIONS

1. Was performed comprehensive study of macro and micro polymeric and straight steel fibers pull-out from the concrete matrix. It was found that all polymeric synthetic fibers break in the concrete, and the cut-off tails are pull-out with friction, the rest straight steel fibers can be fully pulled out, which leads to higher efficiency if comparing to the polymeric fibers.
2. It has been shown that as a result of fiber pull-out from the concrete matrix we observe erosion on the canal surface of the fiber in the concrete, which leads to large spread of force values for fiber pull-out at large inclination angles.
3. As a result of numerical modeling it has been shown that there is a possibility of weak area appearance (contains less concentration of fibers or fibers orientated perpendicularly to the longitudinal axis of the beam). The results of numerical modeling have been confirmed by the X-ray analysis.
4. Analysis of the crack surface has been performed. The coordinates of each fiber have been found on the crack's surface and the diagrams have been built for arrangement of lengths of pulled-out fiber ends and angles to the crack surface.
5. The results of experiments have been used in modeling of beam behavior under load in the mode of the main crack opening.
6. Four numerical models that model the bearing capacity of the beam at the stage of the main crack opening have been developed. Good compliance of experimental and theoretical data at the stage of large openings of the crack has been received.

## REFERENCES

1. Habel K., Viviani M., Denarie E., Bruhwiler E. Development of the mechanical properties of an Ultra-High Performance Fiber Reinforced Concrete (UHPFRC), *Cement and Concrete Research* – 36 (2006), pp.1362-1370.
2. Sekhon JS (2010) Matching: multivariate and propensity score matching with balance optimization, R package version 4.7-11. <http://CRAN.R-project.org/package=Matching>. Accessed 5 April 2012
3. Krasnikovs A., Kononova O., Khabbaz A., Machanovsky E., Machanovsky A.. „*Post – Cracking Behavior of High Strenght (Nano Level Designed) Fiber Concrete Prediction and Validation*”. Nanotechnology in Construction 4th International Symposium”, Agios Nikolaos, Crete, Greece, May 20-22, 2012, pp.1-6
4. Kooiman A. (2000) Modelling Steel Fiber Reinforced Concrete for Structural Design. Ph.D. thesis. Delft University of Technology, CN Delft, Netherlands.
5. Toutanji, H. and Bayasi, Z., 'Effect of manufacturing techniques on the flexural behaviour of steel fiber-reinforced concrete', *Cem. Concr. Res.* 28 (1), 1998, pp. 115-124.

6. R. Gettu\*, D.R. Gardner, H. Saldivar and B.E. Barragfin Study of the distribution and orientation of fibers in SFRC specimens *Materials and Structures* January–February 2005, Volume 38, Issue 1, pp 31-37
7. Edgington, J. and Hannant, D.J., 'Steel fibre reinforced concrete. The effect on fibre orientation of compaction by vibration', *Mater. Struct.* 5 (25) (1972) 41-44.
8. Г.И.Гончаков, Ю.М.Баженов Строительные материалы М.Стройиздат, 1986. 688.стр.
9. Heiko Herrmann, Marika Eik Some Comments on The Theory of Short Fibre Reinforced Materials. *Proceedings of the Estonian Academy of Sciences*, 2011, 60, 3, 179–183
10. А. Н. Зайдель Элементарные оценки ошибок измерений Ленинград, 1968. 25-40 стр.
11. Neville A.M. (1981) *Properties of Concrete*. 3rd ed. New York: Pitman Publishing. 779 p.
12. Виктор Мещерин. Предупреждение трещинообразования в бетоне с помощью фиброармирования. Бетонные изделия. Бетон и железобетон'12 N1 (6) 2012.г.
13. Kononova O., Krasnikovs A., Pupurs A. High Performance Steel Fiber Reinforced Concrete (SFRC) Strength. Prediction and Experimental Investigation, 8th International Symposium on Utilization of High-Strength and High-Performance Concrete, Tokyo, Japan, (2008), pp.543-548.
14. MATLAB Release 7.9, (2009).
15. Fischer G. Structural Applications of Engineered Cementitious Composites (ECC). In: *Ultra-ductile concrete with short fibres: Development, Testing, Applications*, V. Mechtcherine (ed.), ibidem Verlag, pp. 2005, 121 – 133.
16. Krasnikovs A., Kononova O., Eiduks M., Kalinka J., Kharkova G., Galushchak A., Machanovsky A. „*Fiber orientation in viscous fluid flow with and without vibration*”. „*Journal of Vibroengineering*” Volume12, Issue 4, ISSN 1392-8716, Kaunas, Lithuania, December 2010.g, pp. 523-532.
17. Lappa, E. S. *High Strength Fibre Reinforced Concrete: Static and Fatigue Behaviour in Bending*. PhD thesis, Technische Universiteit Delft, 2007.

**Arturs Macanovskis**

**SHORT FIBER COMPOSITE INTERNAL GEOMETRY  
INFLUENCE ON THE MATERIAL'S LOAD BEARING  
CAPACITY AND STRENGTH**

**Summary of Thesis**

---

Registered for printing on 25.04.2014. Registration Certificate  
No. 2-0282. Format 60x84/16. *Offset* paper. 2,00 printing sheets,  
1,32 author's sheets. Calculation 30 copies. Order Nr. 30.  
Printed and bound at the RTU Press, 1 Kalku Street,  
Riga LV- 1658, Latvia.